Daniel Ziesel, BSc

Experimental Setup and Evaluation of MEA Measurements in Organotypic Neuronal Slice Cultures of Neonatal Rats

Master's Thesis

to achieve the university degree of

Master of Science

Master's degree programme: Biomedical Engineering

submitted to

Graz University of Technology

Supervisor

Ass.Prof. Dipl.-Ing. Dr.techn. Theresa Rienmüller

Institute of Health Care Engineering with
European Testing Center of Medical Devices

Head: Univ.-Prof. Dipl.-Ing. Dr.techn. Christian Baumgartner

Graz, September 2019

EIDESSTATTLICHE ERKLÄRUNG

AFFIDAVIT

Ich erkläre an Eides statt, dass ich die vorliegende Arbeit selbstständig verfasst, andere als die angegebenen Quellen/Hilfsmittel nicht benutzt, und die den benutzten Quellen wörtlich und inhaltlich entnommenen Stellen als solche kenntlich gemacht habe. Das in TUGRAZonline hochgeladene Textdokument ist mit der vorliegenden Masterarbeit identisch.

I declare that I have authored this thesis independently, that I have not used other than the declared sources/resources, and that I have explicitly indicated all material which has been quoted either literally or by content from the sources used. The text document uploaded to TUGRAZ*online is identical to the present master's thesis.*

Datum / Date

Unterschrift / Signature

Acknowledgements

I would like to thank everyone who helped me over the course of working on and writing this thesis: the people at the Institute of Health Care Engineering for always lending me a hand when I had questions on compiling my thesis, my colleagues at the Medical University of Graz that provided some of the required samples and materials for the experiments and everyone else who kindly encouraged me in the past months.

I am also very grateful to all my friends, family and girlfriend who supported me during this time. Special thanks goes to my parents, who made it possible for me to conduct my studies in Graz. It has been a wonderful time, I gained many different experiences and made lots of fond memories.

Abstract

The measurement of electrophysiological signals with the help of multielectrode array (MEA) technology can be used for many different practical applications. Samples from neuronal tissue exhibit spontaneous electrical activity and respond to external stimuli in vitro. These signals can be measured by establishing an interface between electrically conducting metal electrodes and the neuronal sample.

The main focus of this master's thesis was to establish an experimental setup for MEA measurements and identify various problems associated with it. The setup comprised several components that were required to ensure the survival of organotypic cultures during experiments. Two MEA measurement systems were tested, the CMOS-MEA5000 and the MEA2100 system by *Multi Channel Systems*. The former uses 4225 electrodes to record signals at very high spatial and temporal resolutions and was utilized in most of the experiments.

A theoretical basis for the measurement with MEA systems and neuronal cultures was compiled. This framework could be used to classify many of the emerging problems and help with the evaluation of measured signals. Efficacious stimulation protocols to evoke electrical activities needed to be researched and implemented. Multiple studies utilizing MEA technology were investigated and compared.

Measurements with organotypic neuronal slice cultures derived from neonatal rats were conducted and the resulting signals recorded. The acquired data was evaluated and different noise sources analyzed. Various improvements to the measurement setup were proposed to ensure the functionality of the established system in the future.

Key Words: MEA, measurement setup, organotypic slice culture, hippocampus, electrical stimulation

Kurzfassung

Die Messung elektrophysiologischer Signale mit Multielektrodenarray-Technologien (MEA-Technologien) hat zahlreiche praktische Einsatzmöglichkeiten. Proben von neuronalem Gewebe weisen in vitro spontane elektrische Aktivität auf und reagieren auf externe Stimulation. Diese Signale können mit Hilfe einer Schnittstelle zwischen elektrisch leitenden Metallelektroden und dem neuronalen Gewebe gemessen werden.

Der Schwerpunkt dieser Masterarbeit lag bei dem Aufbau eines experimentellen Messsystems für MEA-Anwendungen und der Identifizierung verschiedener Problemstellungen, die dabei auftreten könnten. Dieser bestand aus mehreren Komponenten, welche notwendig waren um das Überleben der organotypischen Zellkulturen zu gewährleisten. Zwei MEA-Messsysteme wurden getestet, das CMOS-MEA5000- und das MEA2100-System von *Multi Channel Systems*. Ersteres wurde für die meisten Messungen verwendet und nützt 4225 Elektroden um Signale mit äußerst hoher räumlicher und zeitlicher Auflösung aufzunehmen.

Eine theoretische Basis für das Messen mit MEA-Systemen und neuronalen Kulturen wurde erarbeitet. Mit Hilfe dieser Grundlagen konnten einige der auftretenden Probleme klassifiziert und die gemessenen Signale evaluiert werden. Stimulationsprotokolle zur effektiven Anregung von elektrischer Aktivität wurden recherchiert und implementiert. Mehrere Studien, in denen MEA-Technologien Anwendung finden, wurden untersucht und verglichen.

Die Durchführung von Messungen und die Aufnahme der entstehenden Signale geschah mit organotypischen Gewebeschnittkulturen, welche aus neugeborenen Ratten entnommen wurden. Die aufgezeichneten Daten mussten ausgewertet und die auftretenden Störsignale analysiert werden. Verschiedene Möglichkeiten zur Verbesserung des Messaufbaus wurden vorgeschlagen, um die Funktionalität des etablierten Systems in Zukunft sicherzustellen.

Schlüsselwörter: MEA, Messaufbau, organotypische Schnittkultur, Hippocampus, elektrische Stimulation

Contents

List of Tables

List of Abbreviations

ACSF	Artificial Cerebrospinal Fluid
ADC	Analog-to-Digital Converter
AP	Action Potential
CA	Cornu Ammonis
CMOS	Complementary Metal-Oxide-Semiconductor
CRS	Conditional Repetitive Stimulation
DG	Dentate Gyrus
EC	Entorhinal Cortex
EPSP	Excitatory Postsynaptic Potential
ICA	Independent Component Analysis
IPSP	Inhibitory Postsynaptic Potential
LFP	Local Field Potential
LTD	Long-Term Depression
LTP	Long-Term Potentiation
MEA	Multielectrode Array
MUG	Medical University of Graz
mEPSP	Miniature Excitatory Postsynaptic Potential
PCA	Principal Component Analysis
ROI	Region of Interest
SC	Schaffer Collaterals
Sub	Subiculum

1 Introduction

1.1 Motivation

Multi electrode array (MEA) technology can be used to measure, acquire and process electrophysiological signals from neuronal samples in vitro. Some of these systems offer functionalities to stimulate tissue and record elicited electrical responses. The resulting data can be processed and analyzed further, with the aim to study the propagation of signals through neuronal tissue and the connectivity of stimulable regions. This information could lead to new insights into physiological processes and may be vital for the development of new technologies for the diagnosis and analysis of neurological disorders.

1.2 Problem Statement

In the course of this thesis, a functioning MEA measurement system shall be set up for experiments with two different MEA devices. Therefore, appropriate procedures for MEA measurements have to be researched. Various changes to the system may have to be tested and adapted to establish proper functionality.

To understand the subject matter, a theoretical basis is required. It will serve as a reference for the implementation of the measurement system and the interpretation of the generated data. Studies conducted by other institutions regarding this topic need to be reviewed to gain insight about the usage and capabilities of MEA systems and to compare the collected results.

The main focus of the measurements will be on organotypic hippocampal slice cultures from neonatal rats, but experiments with cortical slices will be conducted as well. Spontaneous activity generated by the neurons themselves, as well as evoked activity caused by stimulation from an external source, shall be investigated. Suitable stimulation protocols need to be defined and implemented. The acquired data must then be processed, before the neuronal activity can be analyzed. Possible signal artifacts need to be examined and solutions for the reduction of interferences proposed.

1.3 Methodological Approach

Organotypic tissue samples from neonatal rats are prepared and maintained by colleagues of the Medical University of Graz. The provided samples are positioned on the electrode area of the measurement chips for the respective MEA system and need to be kept alive during the measurement. Appropriate protocols for the supply of nutrients and oxygen to the sample, as well as suitable temperature conditions need to be considered for the measurement setup.

As a basis, the structure of the rat hippocampus, as well as the neuronal connections within organotypic hippocampal slices need to be understood. The shape of the waveforms that are to be expected from spontaneous and evoked neuronal activity need to be researched in advance. Knowledge about the properties of signal conduction within the sample and between electrodes and tissue serves as a foundation for the analysis of the acquired data.

Once a theoretical framework is established, the measurement system will be set up in a laboratory to conduct the proposed experiments. Several changes to the setup may be required to optimize its performance and the quality of the recorded signals. Furthermore, significant data shall be processed and analyzed to extract parameters of interest. Data acquisition will be done with the software provided for the respective MEA systems.

1.4 Structure of the Work

In the following chapter, important information that is relevant for this work will be compiled and serve as a theoretical framework for further considerations. Some studies that utilize MEA systems to investigate parameters of interest will be featured as well. The next part will lay out the methods that were used in experiments conducted for this work and explore some alternative approaches.

The results of this thesis will be shown in chapter 4, including the setup of the measurement system and some of the acquired data. After that, these results will be discussed and some of the encountered challenges analyzed. The final chapter will give a conclusion to this work and propose some different approaches for future experiments with the tested measurement setups. Some additional information that did not fit into the other chapters will be compiled in the appendices at the end of this thesis.

2 Theoretical Framework

2.1 Neuronal Cultures

There are several established ways to culture neurons for electrophysiological measurements, some of which are discussed in this section. While organotypic slices are easier to prepare and are a good representation of how cells would behave in vivo, dissociated cell cultures can give more specific information about the neurons of interest and the formation of new synaptic connections. In order to understand some of the apparent processes in neurons and neuronal conduction, some basic knowledge needs to be compiled.

2.1.1 Organotypic Slice Cultures

One of the best methods to preserve the function of neuronal cells is the preparation organotypic slice cultures, which show similar characteristics as the organs they originate from. The characteristics of interest for this work are the neuronal conduction of electrical signals and the spontaneous generation of postsynaptic potentials within the tissue. These signals can be measured with the help of patch clamping or mutlielectrode array (MEA) technology and recorded for further evaluation. [MTB+01]

Organotypic slice cultures of neuronal tissue are commonly prepared from the hippocampal formation or the cerebral cortex of animals. They can be obtained by removing the brain tissue in question and cutting it into thin slices under sterile conditions. Frequently used donor animals are neonatal rats or mice of a recommended age between P10 (postnatal day 10) to P12 [Hum15]. At this age, the neuronal tissue already has a sufficient morphology so that individual structures can be distinguished, while still exhibiting good regenerative properties that gradually decrease in older animals.

2.1.2 Organotypic Slice Preparation and Maintenance

After the animal is humanely killed and decapitated, its brain is removed from the skull and the tissue of interest is cut out according to appropriate dissection procedures (e.g. [MTB+01, p.15-16]). A sterile environment is thereby vital to minimize damage to the tissue and prevent cell death. Once the section is separated, organotypic slices

with a thickness of 100 to 400 µm can be cut from it with a tissue chopper, vibratome or rotary slicer [SZI17].

One conventional method to preserve the slice cultures is to carefully transfer them onto a semipermeable membrane insert that was previously placed in one of the wells of a multiwell plate (Figure 2.1B). Depending on their size, up to four slices can be put on each membrane. A culture medium is added below the membrane, which needs to be changed twice per week. The multiwell plate is then placed in an incubator at a temperature of 37 °C and 5 % CO_2 in air. With this technique, the cell cultures can be kept alive for approximately two weeks. [Hum15]

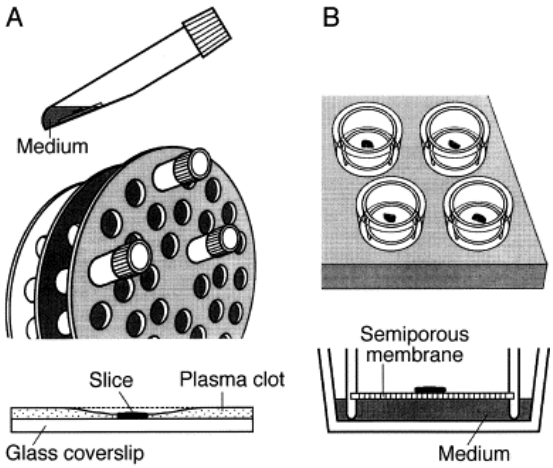

Figure 2.1: Different slice culture preservation methods. (A) Roller-tube technique: The organotypic slice is fixated on a glass coverslip with a plasma clot and placed in plastic tube. The tube is slowly rotated in a rotating mount (ten revolutions per hour) so that the slice culture is covered in medium for half of the time and aerated for the other half. (B) Interface culture technique: The slice culture is placed on a semipermeable membrane which resides on top of a culture medium. The cells are fed through the membrane from one side and aerated with an oxygen mixture containing 5 % CO_2 from the other side. [GCD+97, modified]

Alternatively, slices can be cultivated with methods like the roller-tube technique, where they are attached to a substrate, like a glass coverslip or directly onto the MEA surface, with a droplet of plasma (Figure 2.1A). With these methods, the cultures can survive for longer periods of time and, when cultivated directly on the surface of a MEA chip, do not have to be transferred before every measurement [PSS+11]. However, many of these techniques require special incubators with rotating or tilting mounts to achieve a periodic alteration between feeding and aeration [GCD+97].

2.1.3 Hippocampal Formation and Neuronal Pathways

The hippocampal formation, for the sake of simplicity often called hippocampus, is an elongated structure situated in the medial temporal cortex in both sides of the brain. It is one of the most thoroughly studied neuronal networks and plays a major part in the

consolidation of information to memory and the declarative recollection of memories [PRD+09]. The basic structure is very similar in various mammals such as humans, monkeys and rodents, although they significantly differ in size and volume [AL07].

This work will mainly focus on the hippocampal formation of rats, which is about 100 times smaller than that of a human. When cut into organotypic slices, the cytoarchitecture and neuronal pathways of the hippocampus are mostly preserved, providing ideal samples for electrophysiological measurements [LBP11]. Figure 2.2 shows how different types of hippocampal slices are originally situated in the brain.

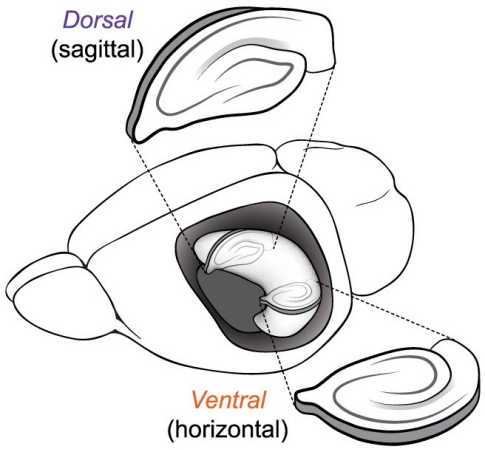

Figure 2.2: Graphic showing the position of the hippocampus in the rat brain and where dorsal and ventral samples originate from in relation to it. [TBT+17, modified]

Its relatively simples structure consists of the hippocampus proper, which can be subdivided into the CA1, CA2 and CA3 regions (cornu ammonis), the dentate gyrus (DG), the enthorinal cortex (EC) and the subiculum (Sub) [AL07]. Figure 2.3A depicts the different regions and how they are connected via neuronal pathways.

In contrast to many other cortical structures, the neuronal connections within the hippocampus are mostly unidirectional instead of reciprocal, meaning that there is no direct return projection between regions. The EC serves as a hub for information leaving and entering the hippocampal formation to and from the neocortex. From there, signals travel through the so-called perforant pathway to the granule cells of the DG and the CA3 region. The DG is connected to the pyramidal cells of CA3 through the unmyelinated mossy fibers, from where they project to CA1 across axons called the Schaffer collaterals (SC). The CA1 region forwards signals towards the EC and the subiculum, which also projects to the deep layers of the EC, closing the loop of hippocampal connections. The diagram in Figure 2.3B shows a schematic representation of all major neuronal pathways within the hippocampal formation. [AL07]

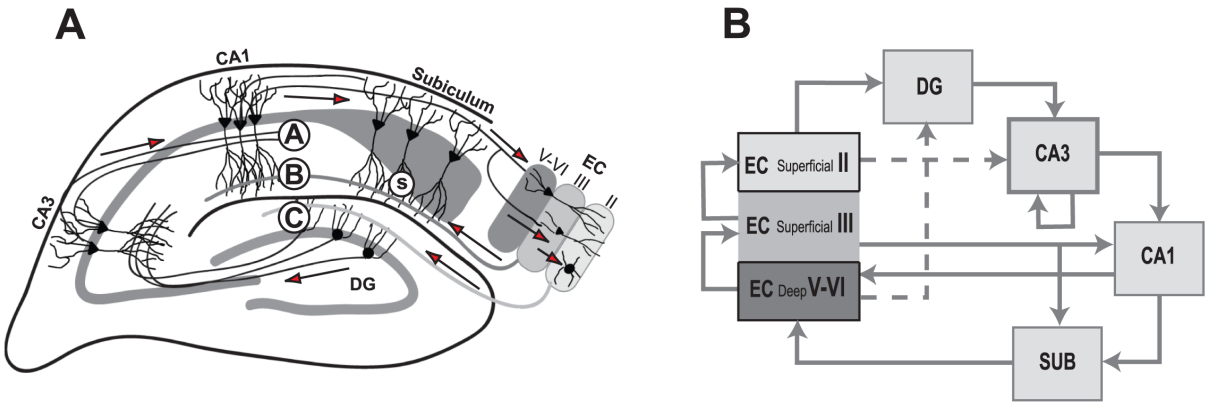

Figure 2.3: Neuronal pathways of the hippocampus. (A) The different regions of the hippocampus: CA1, CA2 and CA3 (cornua ammonis), the dentate gyrus (DG), the enthorhinal cortex (EC) and the subiculum (Sub). Signals are projected along the depicted neurons in the direction of the arrows. (B) Block chart showing how the hippocampal regions are connected and the direction of signal propagation. There is only sparse connectivity along the dashed lines. [DFG14, modified]

2.1.4 Dissociated Neuronal Cultures

Electrical activity in neurons can also be observed in dissociated configurations. To obtain these cultures, neuronal connections in a tissue sample are separated through chemical procedures, leaving only selected cells like dissociated neurons and glial cells suspended in a culture medium. If one wants to work with samples exclusively containing dissociated neurons, other types of cells need to be killed off. Under suitable conditions, these neurons form numerous functional synapses in a two-dimensonal space. Therefore, the formation of axonal and dentritic connections and the basic electrophysiology of neurons can be studied. [PXM13]

Dissociated cultures have many advantages over organotypic cultures and can be kept alive up to several weeks [VWC+04]. They are much easier to visualize under a microscope and particular types of cells can be selected for culturing, providing a highly controlled environment for electrophysiological studies [ND09]. However, their cultivation is not a trivial task and consists of multiple complex steps. A detailed description of the preparation procedure for dissociated hippocampal cultures can be found in [ND09] and [PXM13].

2.2 Electrical Activity of Neurons

Several different effects can lead to electrical activity in neurons. An action potential occurs, when the membrane of a neuronal cell is depolarized above a certain threshold potential. The membrane potential quickly rises and falls back down to its resting state. When an action potential reaches the presynaptic membrane, it triggers the release of neurotransmitters, which in turn causes depolarization or hyperpolarization at the

postsynaptic membrane. A positive potential change is called excitatory postsynaptic potential (EPSP), while a negative change is an inhibitory postynaptic potential (IPSP).

2.2.1 Action Potentials and Neuronal Conduction

An action potential (AP) is the temporary deviation of the membrane potential from its resting state, as shown in Figure 2.4, that can cause the depolarization of adjacent neurons. The explanations in this section are largely simplified and based on the descriptions in [Fle19] and [FJ10].

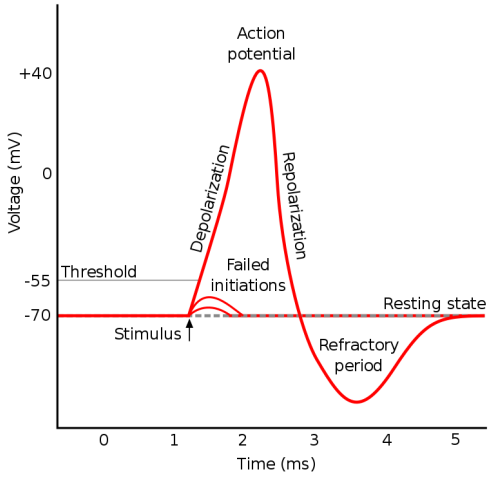

Figure 2.4: Shape of an action potential (AP) with the resting state at $-70\,\mathrm{mV}$ and the threshold potential at $-55\,\mathrm{mV}$. When a stimulus increases the membrane potential above the threshold, depolarization occurs and the voltage rises above $0\,\mathrm{V}$. After approximately $1\,\mathrm{ms}$, repolarization occurs and the voltage drops below the resting potential before returning to the resting state after a short refractory period. [Com16]

The resting potential of the neuronal cell membrane is normally at around $-70\,\mathrm{mV}$, which is measured between the intracellular and extracellular space. This is the result of electrical imbalances and concentration gradients across the cell membrane, as well as different permeabilities of the membrane to distinct ions. If a stimulus depolarizes the cell membrane above a threshold of about $-55\,\mathrm{mV}$, the voltage-gated sodium ion channels open, causing a rapid influx of positively charged sodium ions into the cell. The purpose of this process is to increase the membrane potential to the equilibrium potential of sodium, which is at around $60\,\mathrm{mV}$.

These ion channels, however, are deactivated after approximately $1\,\mathrm{ms}$, when the membrane potential is already well above $0\,\mathrm{V}$. Repolarization occurs, causing the membrane potential to return towards the resting potential through the efflux of potassium ions via voltage-gated potassium channels and leak channels. The equilibrium potential of potassium of roughly $-90\,\mathrm{mV}$ is below the resting potential of the cell membrane.

Due to the delayed inactivation of the potassium channels, the membrane potential is briefly hyperpolarized before finally returning to its resting state.

The next action potential can only be triggered after the membrane potential has reverted to its resting potential, where the voltage-gated sodium channels can be opened again. This time interval is called the absolute refractory period. Although it is possible to trigger action potentials during the subsequent relative refractory period when the cell membrane is hyperpolarized, a greater stimulus is required to reach the threshold potential.

In unmyelinated nerve fibers, the depolarization phase of the action potentials causes an inversion of the local membrane polarity, which in turn leads to a small electrical current flowing in the intracellular fluid between the areas of positive and negative polarity. This current is enough for voltage-gated sodium ion channels in the adjacent section of membrane to open, triggering another action potential which propagates along the length of axon. Due to the refractory period after an action potential, this signal can only travel in one direction, from the axon hillock near the soma to the axon terminals.

In myelinated neurons, the sheath surrounding the axon serves as an electrical insulator and ions can only be exchanged with the extracellular fluid at the nodes between the myelin cells. The electrical impulses therefore jump between the nodes instead of slowly propagating along the cell membrane, leading to a much faster overall conduction speed.

2.2.2 Synaptic Transmission, EPSPs and IPSPs

When an action potential reaches the terminals at the end of the axon, the electrical activity leads to the opening of voltage-gated calcium channels at the presynaptic membrane. The resulting influx of calcium ions facilitates the release of neurotransmitters into the synaptic cleft [HF12]. These neurotransmitters bind to receptors in the postsynaptic membrane, where ligand-gated ion channels are opened to increase the conductance of anions or cations across the membrane, depending on the specific neurotransmitter. An increase in cation conductance leads to depolarization at the membrane and the generation of an EPSP, while a higher anion conductance causes depolarization and therefore an IPSP [FJ10].

An action potential can be evoked through spatial or temporal summation of EPSPs, which themselves have an amplitude in the range of only 1 mV. Spatial summation occurs when EPSPs from multiple nerve fibers arrive at the axon hillock simultaneously, leading to superposition of the two signals and a higher stimulus overall. This sum signal can be decreased by IPSPs, therefore the excitation of an action potential depends on the number of excitatory and inhibitory stimuli. The arrival of a second EPSP before the previous EPSP has fully declined leads to temporal summation, which can also trigger an action potential. [Byr14]

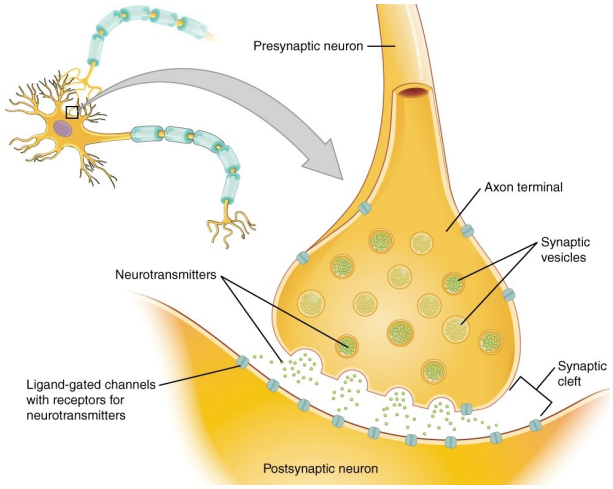

Figure 2.5: Signal transmission at a chemical synapse. When stimulated, the presynaptic membrane releases quantal packets of neurotransmitters into the synaptic cleft, which bind to the receptors of ligand-ganted ion channels at the postsynaptic membrane, prompting them to open. The resulting increase in ion conductance may induce an EPSP or IPSP in the postsynaptic neuron. [Com18]

2.2.3 Spontaneous Activity and Local Field Potentials

Even without evoked activity at the synapses, the postsynaptic membrane may spontaneously release neurotransmitters into the synaptic cleft. This release of single quantal packets of neurotransmitter may lead to miniature postsynaptic potentials, also called mEPSPs or "minis" [She90, p. 365]. Although the amplitude of these mEPSPs is very small compared to evoked EPSPs, they can still trigger action potentials through spatial and temporal summation.

The electrical activity that can be measured in the extracellular space of organotypic cultures or in vivo brain tissue using microelectrodes is called local field potential (LFP) [DB13]. It represents the superposition of synaptic and trans-membrane currents of neurons near the measuring electrode. The electric field of only a small area of tissue is observed, whereby one is more interested in the synchronized electrical input from the surrounding regions than the shape of individual spikes originating from it. Higher frequency signals, such as action potentials, experience much greater attenuation over large distances in the extracellular space than synaptic potentials, which are comprised of lower frequencies.

The difference to an electroencephalogram (EEG) or electrocorticogram (ECoG), where larger measurement electrodes are used, is that the activity of only a small population of neurons is sampled and the measurement is taken in direct contact with the neuronal tissue. The signal components of an LFP may be traced back to the neuronal pathways and neurons they originate from with the help of specialized spike sorting algorithms [RPQ15].

2.3 Stimulated Neural Activity

In order to artificially induce an action potential in the axon of a neuron, parts of the axonal membrane need to be depolarized by changing the potential in the extracellular region. This is usually done by applying a rectangular current pulse between a stimulation electrode near the desired region and a reference electrode in the extracellular fluid. Stimulating pulses are ordinarily several hundreds of microseconds long [VPS+03]. When the membrane potential exceeds a certain threshold as a result of stimulation, an action potential is triggered.

This can be achieved primarily with two different types of stimuli: cathodic or anodic pulses. Furthermore, characteristics of stimulation pulses, the interface between electrode and tissue, as well as a method called long-term potentiation (LTP) will be discussed in this section.

2.3.1 Cathodic and Anodic Stimulation

The following information is mostly gathered from [MBJ05]. For cathodic stimulation, a negative pulse is applied, which leads to the accumulation of negative charges in the extracellular region near the stimulation electrode and the membrane is depolarized. This, however, causes positive charges in the intracellular region to move towards the stimulation site, resulting in hyperpolarization of membrane areas further away from the electrode. With anodic stimulation, a positive pulse is applied to the axonal membrane, hyperpolarizing the region near the electrode. Through the resulting depolarization in areas distant to the electrode, action potentials may occur further away. Anodic stimulation requires more current to trigger an action potential, while action potentials caused by cathodic stimulation may be suppressed by the surrounding hyperpolarized regions.

Cathodic and anodic stimulation can also be used to evoke action potential through a phenomenon called anodic break. When the membrane is hyperpolarized and then suddenly returns to its resting potential, sodium conductance may be increased for a short period of time. If the inactivation of sodium channels is delayed long enough, the membrane potential may increase above the threshold potential, triggering an action potential.

2.3.2 The Electrode-Electrolyte Interface

In order to excite neural tissue, there needs to be an interface between the conduction of electrons in an electrode and the ionic conduction in the extracellular fluid, which is often denoted as the electrolyte [BG13]. The simplified electrical model of this interface is a circuit consisting of an impedance in parallel to a capacitor, as shown in Figure 2.6(b).

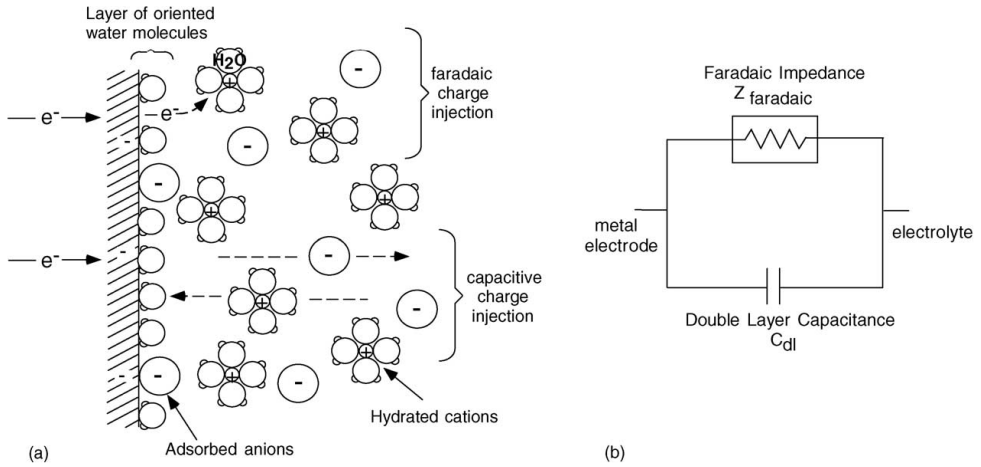

Figure 2.6: The interface between electrode and extracellular fluid. (a) The chemical and physical processes at the interface, comprised of Faradaic and capacitive charge injection. (b) The simplified electrical model of the electrode-electrolyte interface. [MBJ05]

Primarily, there are two effects taking place at the interface between the working electrode and the electrolyte: the capacitive redistribution of charge and Faradaic charge transfer [MBJ05], as depicted in Figure 2.6(a). When a potential is applied to the electrode, ions of opposite charge move towards it and form a capacitive layer at its surface, while species with the same polarization are repelled. The movement of ions in the electrolyte elicits the flow of an electric current between the working electrode and a counter electrode in the electrolyte. This effect can be modeled by a simple capacitor called the double layer capacitance C_{dl}, which is directly proportional to the surface area of the electrode [BG13].

Due to electrochemical reduction and oxidation reactions at the surface of the electrode when it is driven negative or positive, electrons move into the electrolyte, resulting in electric current flow. This Faradaic transfer of charges may be irreversible and can form unwanted products in the electrolyte that may need to be removed. The effect of charge dissipation is representend by the Faradaic impedance $Z_{faradaic}$ [MBJ05].

2.3.3 Stimulation Pulses

The minimal required current strength for sufficient stimulation depends on the length of the applied impulse. This relationship is depicted in the strength-duration curve in Figure 2.7. When the pulse is applied for a longer time, a smaller amplitude is needed to evoke an action potential and vice versa. The rheobase current I_{rh} is the minimal current strength that can trigger an action potential for a pulse of infinite duration and depends on the distance between the electrode and the target membrane [MB09]. The Chronaxie T_{ch} is the length of a current pulse that has twice the amplitude of the rheobase current. The shape of the strength-duration curve, and therefore also the chronaxie, is different depending on the type of excited tissue.

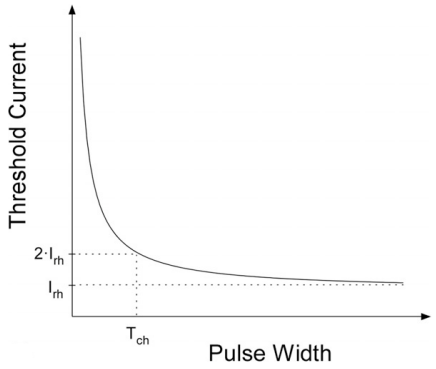

Figure 2.7: The strength-duration curve shows the relationship between current strength and length of a stimulation pulse that is sufficient for the excitation of an action potential. Its shape and parameters are characteristic for different kinds of tissue. [BG13, modified]

Different shapes of commonly used stimulation pulses are shown in Figure 2.8. The type of pulse has an effect on the efficiency of action potential excitation and possible damage to the tissue, as well as corrosion of the electrode itself. The effects of various stimulation pulse types are discussed in great detail in [MBJ05]. Generally, charge-balanced biphasic current pulses with a short interphase delay are preferred in order to prevent loss of excitability over time, since monophasic stimulation may cause irreversible changes at the electrode surface during periodic pulsing [MB09]. The reversal phase of the biphasic pulse is necessary to compensate the electrochemical processes caused by the stimulation pulse and is normally applied after a short delay to prevent immediate hyperpolarization [MBJ05].

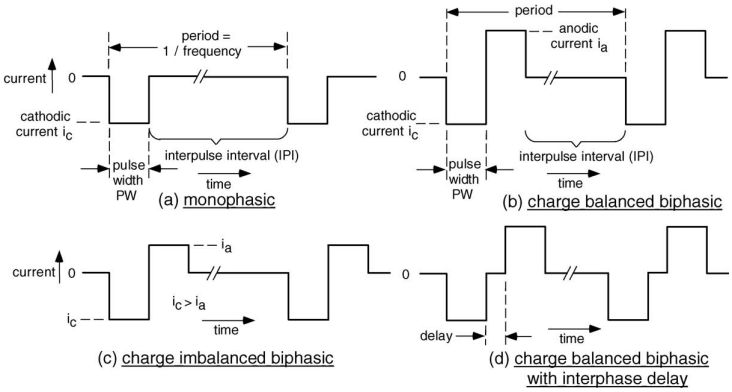

Figure 2.8: Examples of commonly used cathodic stimulation pulses. [MBJ05]

2.3.4 Long-Term Potentiation

Through stimulation with a train of pulses over a short period of time, the strength of synaptic connections in a sample can be increased [CSGR06]. This effect is called long-term potentiation, or LTP in short. These strengthened connections are more

likely to spontaneously release neurotransmitters into the synaptic cleft and express increased EPSP amplitudes [Sch97]. Several different stimulation waveforms can be applied to achieve this effect.

A single train of pulses, for example, can induce LTP that lasts one or two hours, while multiple pulse trains may cause long-lasting LTP enduring for several hours [CSGR06]. Synaptic connections can also be weakened leading to so-called long-term depression (LTD), which can be achieved via stimulation with longer monophasic current pulses [WHG02].

2.4 Multielectrode Array Technology

State-of the-art multielectrode array (MEA) chips are comprised of tens to thousands of single electrodes, depending on the utilized technology, that are integrated in a substrate. These electrodes are often aligned in an evenly spaced grid with a size of only a few square millimeters, which facilitates the two-dimensional measurement of the electrical signals in tissue samples placed on the chip surface. Conventional MEAs with an electrode spacing of 200 µm are commonly used for experiments with neuronal cell cultures, while newer CMOS-MEA technology allows for much higher spatial resolutions down to the subcellular level [MAA+18].

2.4.1 Principal Structure of Conventional Multielectrode Arrays

Conventional MEAs are passive devices, where a conducting material is deposited on a substrate through photolithographic processes and then covered by an insulating layer. The insulating layer near the electrodes is removed to enable transition of electrical signals exclusively at these sites. An example of what the surface of an MEA chip looks like is shown in Figure 2.9 (top left). Electrodes on MEA chips - like the ones designed by *Multi Channel Systems* - are often aligned in an 8x8, 12x12 or 16x16 grid, with an electrode diameter of 8 µm to 30 µm and an inter-electrode spacing between 30 µm and 200 µm.

Through on-chip wiring, the electrical signals detected at each electrode are conducted to exterior circuitry, where they are individually amplified and filtered as depicted in the block diagram in Figure 2.9 (top right). The signals are then aggregated and captured with an acquisition board that can send the collected data to a computer for further processing and analysis. Data is recorded from all electrodes in the grid simultaneously, with sampling rates of up to 50 kHz.

Stimulation is often applied through the same electrodes through which signals are measured. With such a setup, the electrodes may need to be briefly disconnected from the amplifiers during the application of stimulating pulses to prevent the recording of

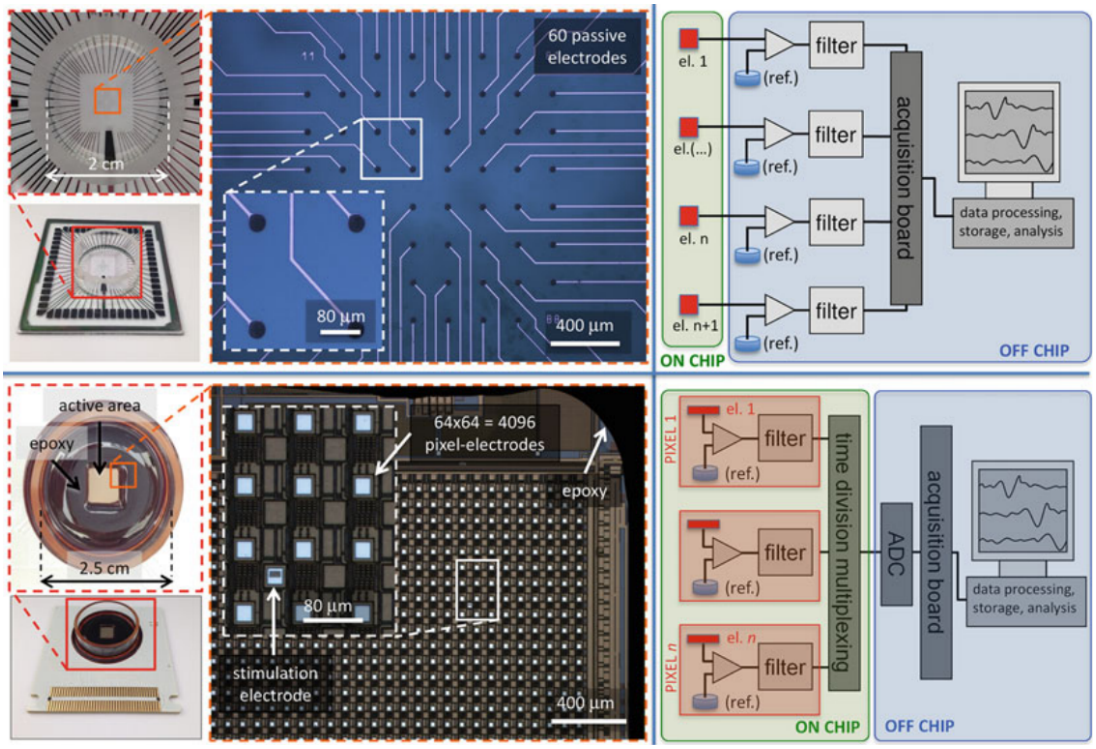

Figure 2.9: Examples for conventional MEAs and high-resolution CMOS-MEAs with schematic illustrations of their integrated recording circuits in the right column. (top) A passive, 60-electrode MEA with electrodes aligned in an 8x8 grid (60MEA200-series by Multi Channel Systems GmbH). (bottom) An active CMOS-MEA chip with 4096 recording electrodes in a 64x64 grid with 16 interspersed stimulation electrodes (HD-MEA Stimulo by 3Brain AG). [MAA+18]

stimulation artifacts. An external electrode in contact with extracellular solution often serves as a reference for the measured voltage.

2.4.2 High-Resolution Multielectrode Arrays

CMOS-based MEAs are active devices and facilitate the acquisition of signals from several thousand electrodes at the same time, resulting in a very high spatial resolution. The electrodes are often only a few micrometers wide and are spaced some tens of micrometers apart from each other, as shown in the example chip in Figure 2.9 (bottom left).

Since direct wiring of every single electrode connection would be nearly impossible at that scale, signals are amplified and filtered close to the electrode and connected to the off-chip circuitry via a common signal path. Spatial attribution of signals of individual electrodes is realized through time-division multiplexing. This method involves an alternating switch-matrix, through which signals from each electrode are only allowed to pass to the data acquisition element for a short amount of time. Analog-to-digital

conversion (ADC), further data accumulation and signal processing is performed off-chip as depicted in Figure 2.9 (bottom right).

There are multiple different ways to measure signals with electrodes at such a small scale, two of which are presented in Figure 2.10. In one method, the electrolyte is capacitively coupled to the metal electrodes through a thin dielectric layer that was applied to the electrode surface (Figure 2.10A). The electrodes are connected to sensing transistors embedded in the CMOS chip, which also serve as a signal amplifier [ZJC+17].

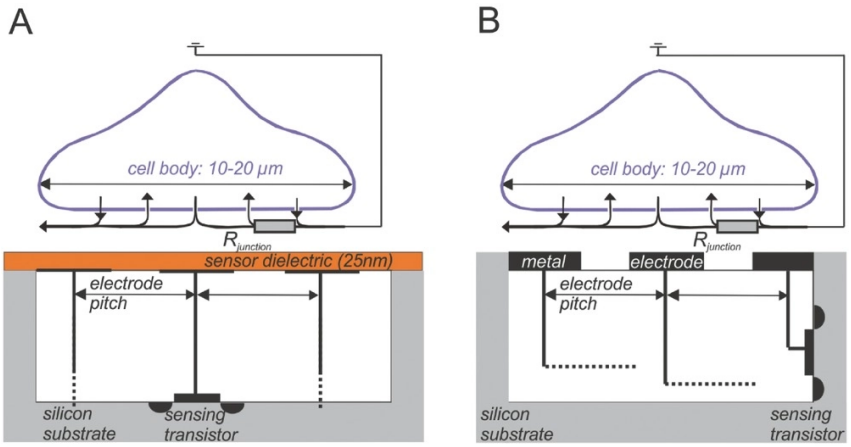

Figure 2.10: Different implementations of CMOS-based MEAs. (A) A thin dielectric layer facilitates capacitive coupling between metal electrodes and electrolyte. (B) The metal electrodes are in direct contact with the electrolyte. $R_{junction}$ is the resistance between the dielectric and the cell membrane and affects the signal quality. [ZJC+17]

Figure 2.10B shows a configuration where metal electrodes are in direct contact with the extracellular fluid. The connected sensing transistors are spatially separated from the electrodes to ensure stability over a longer period of time [FEH+09]. A detailed comparison between different types of CMOS-MEA implementations is reviewed in [ZJC+17].

CMOS-MEAs conventionally have separate electrodes for stimulation, which are located in the spaces between the measuring electrodes (Figure 2.9 (bottom left)). This has the advantage that the influence of stimulation artifacts on the measurement is negligible and no decoupling is necessary.

2.5 Training of Neurons

As shown in several studies, neuronal cultures can be trained [Sch97, SLMR09, OKMS16, HFY+18]. The basic principle of this concept is that neurons are stimulated through an electrical or chemical input in order to strengthen or establish certain connections between them. The improved connectivity can manifest in the form of an

increased rate of spontaneous activity or through a changing shape of the stimulus response. These signals are measured and interpreted as a specific stimulus-response, which can be used to encode basic commands. Effectively, training of neurons could be utilized as a simple computing unit to control operations of external devices [HFY+18].

[OKMS16] used high-frequency stimulation to change the plasticity of neuronal networks. They were able to induce long-term potentiation (LTP) and long-term depression (LTD) in cortical neurons with an MEA system. The application of 20 trains of bipolar pulses at a frequency of 10 Hz, 120 times in 4 s intervals, lead to long-lasting LTP and a significant increase in spike activity for more than 24 hours. With a different stimulation protocol, spike activity was considerably decreased through LTD. It is apparent that the frequency of spontaneous neuronal activity can be artificially manipulated for a period of several hours after electrical stimulation.

In [SLMR09], researchers used current pulses to periodically stimulate dissociated neurons with the help of an MEA system. A so-called conditional repetitive stimulation (CRS) algorithm, which was proposed in [SM01], was implemented. By probing different stimulation sites, they evaluated which electrodes could elicit the best stimulus-response. It was noticed that when these selected sites were stimulated, the number of stimuli required to evoke the same response gradually decreased. Not only that, but the properties of the whole network changed over time to incorporate this specific stimulus-response. This shows that the interconnections of a neuronal sample could be changed on a physiological level just through the application of electrical stimuli.

The researchers in [HFY+18] take this concept even further and discuss practical applications for the techniques mentioned above. A network of neurons can be conditioned and its plasticity changed so that a stimulus elicits a desired response depending on its location and the shape of its waveform. By building an interface between this network of biological neurons on an MEA chip and a computer, one could use them to compute and control simple devices. Eventually, these trained neurons might be able to solve more difficult computational problems through novel learning algorithms.

3 Methods

This chapter aims to explain the basic methodologies used for MEA measurements, which includes the setup of the MEA system itself, the acquisition of signals, electrical stimulation and analysis of recorded data, and put them into a context that can be applied in practice. If not marked otherwise, most of the information below was gathered from the manuals of the CMOS-MEA5000 and MEA2100 systems, as well as the corresponding application notes provided on the website of *Multi Channel Systems*.

3.1 Measurement Setup

The setup for the measurement of electrical signals from neurons on MEA systems consists of three main components: one system to control the temperature of the sample, a system for the supply of nutrients and oxygen, as well as several data pathways for the acquired data and the communication between systems. Each of these components is crucial to the survival of neuronal samples and to attain correct and relevant signal measurements.

A basic measurement setup for the recording of electrical signals from organotypic slice cultures is shown in Figure 3.1. The cultures are nourished through a perfusion system that supplies a continuous flow of artificial cerebrospinal fluid (ACSF), which is eventually collected in a waste container. The temperature of the perfusion solution, as well as the temperature of the MEA chip, are adjusted through a temperature controller connected to respective heating elements. A sensor meanwhile ensures that the temperature at the surface of the chip remains at the preset level. Data generated by the MEA system is sent to a PC for further processing and analysis. The PC also communicates with the temperature controller and sensor, as well as the MEA system to adjust specific parameters.

The perfusion system is not required for measurements with dissociated neural cultures and certain types of organotypic cultures. These samples are grown directly on the chip and can survive for short periods of time outside an incubator in cell culture medium, as long as the MEA chip itself is heated. Most parts of the setup are identical for the utilized MEA and CMOS-MEA systems.

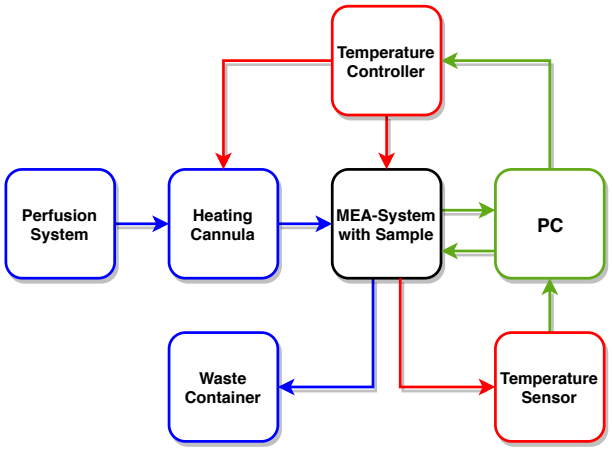

Figure 3.1: MEA-measurement setup for organotypic slice cultures. The pathway of the perfusion solution (blue), the systems for temperature control and measurement (red), and the data connections (green) are shown.

3.1.1 Samples

Neuronal culture samples are often extracted from rodents like rats or mice that are only a few days old. For the experiments in this work, P5 samples are extracted from neonatal Sprague Dawley rats, a breed of laboratory rats commonly used for medical research. Organotypic slices are prepared with a tissue chopper as described in Section 2.1.2 and transferred onto semipermeable membranes, with multiple samples on each culture plate of a 6-well plate.

Before the measurement is started, a small section of membrane is cut out around the desired sample with a scalpel. This segment is then inverted and placed in the center of the MEA chip, so that the tissue is in direct contact with the measurement electrodes. The transfer has to be carried out quickly, since the neuronal cells may die off after approximately one minute without culture medium or the perfusion supplying nutrients and oxygen.

3.1.2 Heating System

In order to provide a physiological environment for neuronal samples, they are usually kept at a temperature of around 32 °C during MEA measurements. To achieve this, the fluid stream and the MEA chip need to be heated. A perfusion cannula with an integrated heating element is utilized to adjust the temperature of the perfusion solution, while a heating plate in the MEA system warms the chip to the desired temperature.

Both of these devices communicate with the temperature controller that is connected to a PC, from where the temperature can be adjusted to an appropriate value. To ensure

the stability of the configured values, an infrared sensor measures the temperature data and sends it to the PC as well. These systems are shown in red in Figure 3.1.

3.1.3 Buffer Solution

As previously mentioned, organotypic slice cultures need a biological buffer to sustain physiological electrical activity for several hours [BVE+15]. Artificial cerebrospinal fluid (ACSF) is a commonly used buffer solution that provides neuronal samples with oxygen and maintains a physiological pH level and osmolarity, as well as supplying glucose as a source of energy.

Bicarbonate (HCO_3^-) or HEPES are often used as base buffers for ACSF. HEPES-based buffers must be bubbled with pure oxygen before and during use, while bicarbonate buffers require carbogen, which is a mixture of 95 % oxygen and 5 % carbon dioxide. An example for a bicabonate-based ACSF buffer is given in Table 3.1, while the recipes for several additional ACSF solutions are compiled in Appendix A.1.

Compound	**Conc. [mM]**	**M.W.**	**g/1L 10x Stock**	**g/2L 10x Stock**	**g/500mL ACSF**	**g/1L ACSF**
NaCl	125	58.44	73.050	146.100		
KCl	3.5	74.55	2.609	5.219		
$NaH_2PO_4 \cdot 2H_2O$	1.2	156.01	1.872	3.744		
$CaCl_2 \cdot 2H_2O$	2.4	147.01	3.528	7.056		
$MgCl_2 \cdot 6H_2O$	1.3	203.30	2.643	5.286		
$NaHCO_3$	26	84.01			1.092	2.184
Glucose$\cdot H_2O$	25	198.17			2.477	4.954

Table 3.1: Bicarbonate ACSF-Buffer from the MEA application note for organotypic cultures (provided by Multi Channel Systems GmbH).

Stock solutions without glucose, bicarbonate and HEPES can be prepared in advance and last for approximately one month. The remaining components have to be added last, after which the final ACSF should be consumed within one day. After bubbling the buffer with the respective gas, the pH value can be adjusted to a physiological level of pH 7.4 by successively adding small amount of NaOH and measuring the pH after mixing. The ACSF buffer shall be bubbled continuously during use to ensure a constant supply of oxygen to the cells in the tissue sample.

3.1.4 Perfusion System

A perfusion system is employed to facilitate a consistent flow of ACSF across the surface of the MEA chip so that the tissue sample is continuously supplied with oxygen and

nutrients during measurements. There are several different types of perfusion systems with active and passive pumping mechanisms.

One commonly used method is to utilize the potential energy of the fluid in an elevated reservoir with an opening at the bottom to push the perfusion solution through a series of tubes with the force of gravity. The ACSF buffer should flow into the culture chamber at a rate of 2 to 5 ml/min, which can be adjusted by clamping the influx tube. It is removed through a suction tube on the other side of the culture chamber, which is connected to an active pumping system, and finally collected in a waste container. The pathway of the perfusion solution is depicted in blue in Figure 3.1.

It is important to note that the perfusion system can introduce unwanted interferences to the measured electrical signal. These can express as low frequency noise, which originates from the fluid level varying due to uneven suction. It can be eliminated by changing the position of the tubes, adjusting the suction rate or retrospectively via high-pass filtering. Another kind of interference is in the shape of localized spikes in the area near the influx tube due to the change in conductivity when a small air bubble moves between the sample and the MEA surface. This effect can be diminished by improving the contact between sample and MEA surface through even application of small amounts of mechanical pressure during the measurement or by adjusting the position of the influx tube.

3.1.5 Reference Electrode

To provide a stable reference for the potential measured at the working electrode, an external reference electrode is connected to the ground of the internal amplifiers of the MEA system. The other end of the electrode, which is usually an Ag/AgCl-electrode, is positioned in the bath solution. One has to make sure that the fluid level is not reduced below the position of the electrode, which could lead to sudden disconnections and result in erratic noise fluctuations.

3.1.6 Fixation of Organotypic Slices

In order to prevent movement of organotypic slice cultures during a measurement, which may be caused by the surface tension of the flowing perfusion, they need to be fixated. A good method to achieve this is to place a slice grid on top of the tissue sample that was positioned on the MEA chip. Slice grids are often constructed specifically for certain MEA chip types and sample sizes by fixating nylon threads to a horseshoe-shaped piece of biocompatible material such as titanium. This construction allows the perfusion to flow evenly across the sample, while facilitating the application of uniform pressure to hold the slice down.

If the weight of the slice grid is not sufficient to hold the sample down on its own, small weights can be placed on top of it. Alternatively, the slice grid can be held down

with a micromanipulator, with which the amount of pressure enacting on the sample can be adjusted in small increments.

A higher pressure reduces the gap between slice and MEA chip, which leads to better conductivity between the two mediums and subsequently to a higher signal amplitude and signal-to-noise ratio. It also decreases interferences from the entry of air bubbles into the gap and hinders signal conduction between electrodes through the medium, allowing for better localization of neuronal spikes. However, the experimenter needs to be careful when applying force to the sample, since an excessive amount may cause damage to the cells.

3.1.7 Chip Coating

The attachment between neuronal cultures and MEA chips is relatively poor due to their smooth surface and the high hydrophobicity of their materials, especially for chips based on CMOS technology. To increase the attachment and improve the environment for cellular growth, the chip surface can be coated with standard coating protocols. Coating with nitrocellulose solution, for example, is a quick and simple procedure, allowing the sample to stick to the surface of the chip.

Nitrocellulose stock solution is prepared by dissolving a $1\,mm^2$ piece of nitrocellulose membrane in 10 mL of methanol. The final solution is obtained by mixing the stock solution with methanol in a 1:10 ratio. This nitrocellulose solution is then applied by pipetting small amounts (3 to 5 µL) onto the surface of the chip and letting it dry for a few seconds.

3.1.8 Visual Inspection

Samples can be visually inspected to evaluate their texture and quality, and to ascertain their position in relation to the electrodes of the MEA chip after they have been transferred onto it. An example picture of a rat hippocampal slice on top of a membrane sheet, taken by a digital microscope camera through a reflected-light microscope, is shown in Figure 3.2. Preferably, samples are photographed before a measurement so that the experimenter knows where to stimulate the tissue and what electrical response is to be expected.

However, this approach poses a problem with organotypic slice cultures. They have to be observed under a microscope before perfusion is started, since otherwise the sample may move later on during the measurement. One solution would be to position the MEA system itself on top of the movable stage of the microscope. A picture can be taken directly after the slice is transferred to the MEA chip and the perfusion is started as soon as possible. Another approach would be to employ slice fixtures that allow a clear view of the sample during the measurement. This, however, would not work for light-sensitive CMOS-MEA chips.

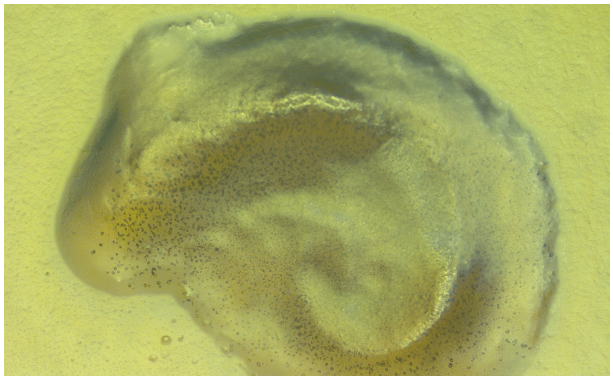

Figure 3.2: Organotypic hippocampal slice from a P5 rat viewed under a reflected-light microscope.

Some MEA systems with transparent chips are constructed with a viewing window at the bottom, where the sample can be looked at with an inverted microscope during the measurement while being held down from the top. Samples that do not require perfusion are easier to observe visually, since they normally do not move during the measurement.

3.2 MEA Measurement Systems and Chips

In the course of this thesis, two MEA systems were available for experiments: the CMOS-MEA5000 and the MEA2100 system, both by *Multi Channel Systems GmbH* which is based in Reutlingen, Germany. These devices will be described and compared in this section.

3.2.1 CMOS-MEA5000

The CMOS-MEA5000 uses CMOS technology to achieve a very high spatial resolution for electrophysiological measurements. The system consists of an interface board connected to a PC via an USB 3.0 interface and a headstage, which is the core of the system and is shown in Figure 3.3A. The CMOS-MEA chips are mounted in this headstage, which samples data from the chip at up to 25 kHz. It also carries out analog-to-digital conversion with 14 bit resolution, amplifies the signals and provides three different stimulus generators.

An example of a CMOS-MEA chip with a culture chamber is shown in Figure 3.3B. Different types of chips are available for recordings with slice cultures or dissociated cultures, as well as chips with grooves in the culture chamber to achieve a more laminar perfusion flow. To mount a chip, the headstage is opened up and the chip placed in its center, after which it is closed again so that the chip is wedged between the contact electrodes at the top and the heating plate at the bottom.

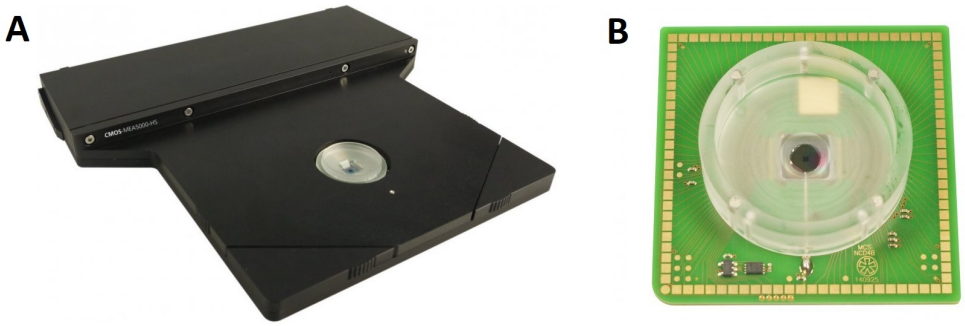

Figure 3.3: Components of the CMOS-MEA5000 system by *Multi Channel Systems GmbH*. (A) The CMOS-MEA5000 headstage, which samples and converts data, amplifies signals and generates electrical stimuli. (B) A CMOS-MEA16-CC chip with a culture chamber for recordings with dissociated cell cultures. Recording Electrodes are arranged in a 65 by 65 grid with an inter-electrode distance of 16 µm and a total chip area of 1 mm^2.

Chips are available with 16 µm and 32 µm inter-electrode distances. Recording electrodes are arranged in a 65 by 65 grid with an interspersed grid of 32 by 32 stimulation electrodes. Therefore, there are a total of 4225 recording electrodes and 1024 stimulation sites in a 1 mm^2 or 4 mm^2 area. The center of the chip is coated with a planar oxide to increase biocompatibility. The electrodes are capacitively coupled to the electrolyte of the sample, as explained in Section 2.4.2. Figure 3.4A depicts a schematic drawing of the electrode arrangement and the chip surface observed under a microscope is shown in Figure 3.4B.

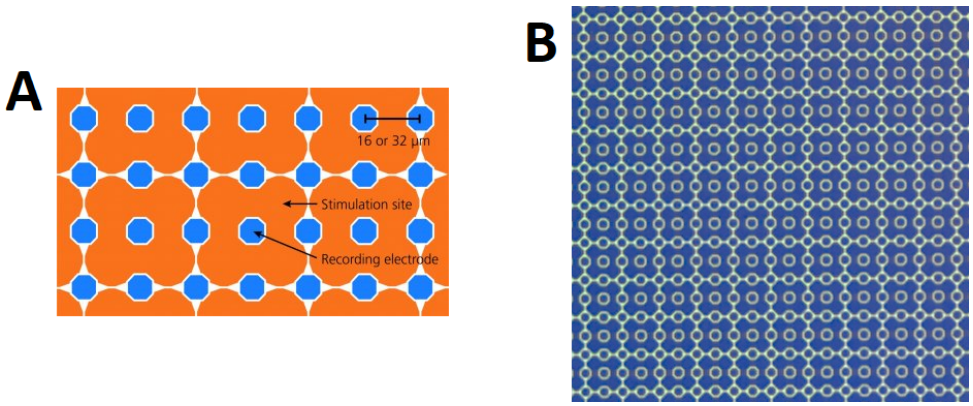

Figure 3.4: Electrode surface of a CMOS-MEA chip. (A) Schematic drawing showing stimulation and recording electrodes and the inter-electrode distances. (B) Picture of the surface of a CMOS-MEA16-CC chip, taken under a reflected-light microscope.

The integration of dedicated stimulation electrodes facilitates continuous signal measurement while electrical pulses are applied. Only positive voltages can be utilized for stimulation, whereby a positive or negative voltage ramp induces a respective positive or negative current pulse. To prevent damage to the chip, only charge-balanced, biphasic pulses starting with a positive pulse may be induced. A minimum of nine stimulation electrodes is required for effective neuronal stimulation.

CMOS-MEA chips can be reused and need to be cleaned between measuring different samples to remove all cells and contaminants remaining on its surface. A simple way to achieve this is to apply 70 % ethanol to the culture chamber, wiping the chip surface with a cotton swab and letting it dry for a few minutes. Protocols for more thorough cleaning suggest submerging the entire chip in a beaker with cleaning detergent for two hours, before rinsing it with distilled water. If defect contacts are detected in the recording software, the metal connections at the edge of the chip can be wiped with 70 % ethanol to restore proper electric conduction to contact pins on the headstage.

Even though the CMOS-MEA5000 system allows for much higher spatial measurement resolutions than the MEA2100 system, it has some major disadvantages. For one, the CMOS chips need to be calibrated with an automated tool before use, which is accompanied by problems with varying signal offsets. The calibration step also needs to be considered when determining the order in which parts of the measurement system are set up. Since CMOS chips are active devices, they need to be powered down before taking them out of the headstage, otherwise their electronics may be damaged. CMOS technology is also sensitive to light, therefore the chip needs to be covered with an opaque lid several minutes before calibration and during measurements to achieve stable light conditions. Another problem is that samples on the chip can only be looked at from the top during measurements, which makes visual inspection with a microscope difficult. Due to the high spatial and temporal resolutions of the recordings, large amounts of data of more than 100 megabytes per second are generated, which can be difficult to store and analyze. Therefore, powerful PCs are required to perform sufficiently fast data operations.

3.2.2 MEA2100

While the MEA2100 system has a much lower spatial measurement resolution than its CMOS-counterpart, it is not subject of many of the problems arising with the use of CMOS technology due to its relative simplicity. The adjustable sample rate of the system can be set to a maximum of 50 kHz, allowing for an even higher temporal resolution. Its headstage, which provides similar functionalities as the headstage of the CMOS-MEA5000 system, can be connected to the same interface board for communication with a PC. It is smaller in size than the CMOS-MEA5000 and has a transparent viewing window at the bottom. Therefore, samples can be looked at with an inverted microscope while measurements are conducted, without slice fixtures obscuring the view.

The chips themselves are transparent and are fabricated as described in Section 2.4.1. An example chip is shown in Figure 3.5A, where the contact pads and their connections to the central chip area can be identified. The electrode area is framed by a plastic ring, which keeps the perfusion solution confined to the central area. Figure 3.5B depicts how the electrodes are arranged on the chip, and Figure 3.5C shows what the electrode area looks like under a reflected-light microscope.

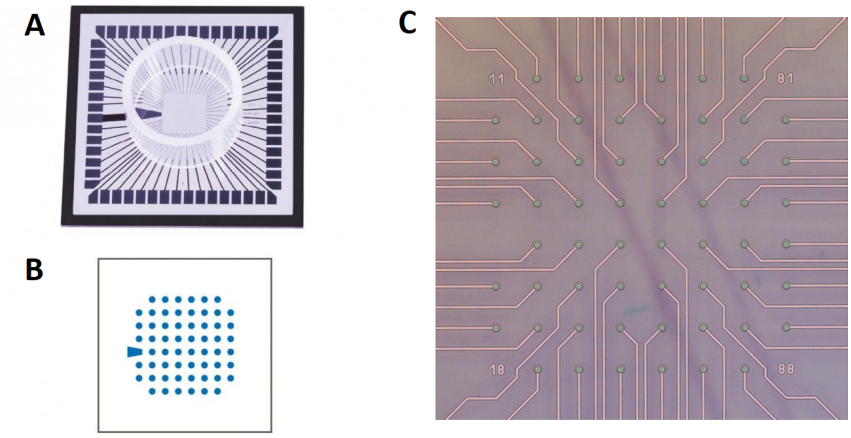

Figure 3.5: The 60MEA200/30iR-Ti chip for the MEA2100 system. (A) Illustration of the whole chip showing contact pads and connections to the measurement electrodes. (B) Electrode arrangement in an 8 by 8 grid with missing corner electrodes. (C) Picture of the electrode area taken with a reflected-light microscope.

Chips for the MEA2100 system are available with a total of 32, 60, 120 and 256 electrodes. For testing purposes in this work, chips with 60 electrodes were utilized. The electrodes are arranged in an 8 by 8 grid with a spacing of 200 µm between them and the corner electrodes missing. Recoding and stimulation protocols utilize the same electrodes, which is why data acquisition is briefly disabled when stimulation pulses are applied.

The same cleaning protocols used for CMOS-MEA chips can be employed for the reusable MEA2100 chips. They do not have to be calibrated before the measurement and show no sensitivity to light, making them much easier to handle. They also generate a significantly smaller amount of data, which allows for easier and quicker data analysis. The spatial measurement resolution, however, is much lower than that of the CMOS-MEA5000 system, making it difficult to identify individual neurons in the recorded data.

3.3 Signal Recording

Signals of both MEA systems can be recorded with accompanying software packets that provide similar functionality. The CMOS-MEA5000 uses a program called *CMOS-MEA-Control* and the MEA2100 is controlled by the *Multi Channel Experimenter*. They let the user adjust the sampling rate, bandwidth and signal range of the system, select the desired measurement area to reduce the amount of stored data and facilitate the introduction of different stimuli to selected electrodes. During measurements, various interferences and noise sources may affect the signal, which have to be filtered out or reduced by adjusting the measurement setup.

3.3.1 Data Acquisition

The measurement software of MEA systems displays measured signals in real-time and provides functions to record and store the acquired data. With the CMOS-MEA5000, the measured signals can be viewed in the form of a heatmap, where the x- and y-axis correspond to the electrode position on the chip and the signal amplitude is represented by colors. The heatmap can also be configured so that the colors represent the frequency of occuring spikes at any given position. A smaller number of electrodes can be selected, from which electrical signals are displayed in a separate window with time on the x-axis and voltage on the y-axis. For the MEA2100, which acquires signals from a significantly smaller number of electrodes, all signals are displayed in the same window simultaneously. In both programs, single electrodes may be selected for a detailed view of the acquired signal.

Data recording can either be started manually or coupled to a stimulus signal with a trigger. The recording can be set to last until a preset amount of time has passed, another trigger occurs or until it is manually stopped. It is advised to log the parameters of each experiment in a measurement protocol, an example of which can be found in Appendix A.2. Parameters of interest may be the time and date of measurement, the type, age and source of the sample, the perfusion solution that was used or the shape and location of an applied stimulus. Recorded data can later be analyzed more thoroughly with different software packets.

Both systems include test chips to try out different functionalities of the MEA systems in a controlled environment. With these chips, noise levels and internal stimulation can be tested, as well as the calibration of the CMOS-MEA5000 system. The MEA2100 system also comes with a test signal generator, which is powered by a battery and can output a variety of different signals that may be acquired by the headstage like from any other chip. Two example signals, an EPSP of an organotypic hippocampal slice and spikes from hippocampal neurons, are shown in Figure 3.6.

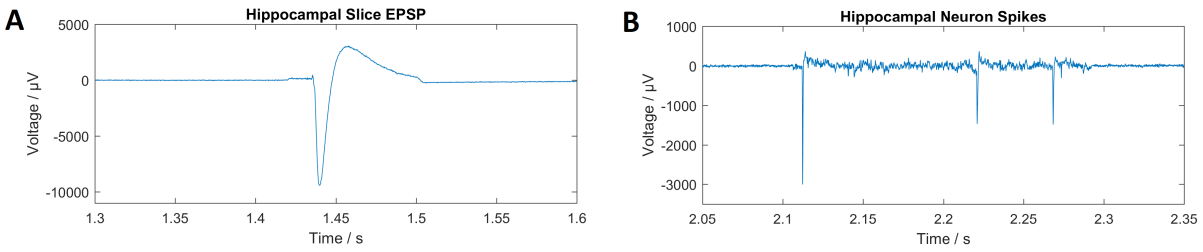

Figure 3.6: Example signals acquired from the signal generator test chip of the MEA2100 system. (A) An EPSP produced by the neurons in a hippocampal slice with a large preceding inhibitory spike. (B) Spontaneous spikes from dissociated hippocampal neurons.

These signals are a good representation of the shapes and amplitudes that they would exhibit in a real measurement. The data was recorded and exported from the *Multi Channel Experimenter* software and then imported and displayed in *Matlab*. The different

signal shapes that can theoretically be measured with an MEA system are described in Section 2.2.

3.3.2 Interference and Noise

Different forms of interferences and noise can affect signal quality or even be mistaken for spontaneous neuronal activity. It is therefore of interest to reduce the noise amplitude and remove interferences as effectively as possible. The noise level of the CMOS-MEA5000 system is usually between 300 and 400 µV, while a noise level of about 20 µV is normal for the MEA2100. Predominantly, there are three different external noise sources affecting the signal that is measured from neuronal samples: power line noise, perfusion noise and bubble artifacts.

Power line noise with a frequency of 50 Hz may be picked up by the perfusion system and electrodes through capacitive coupling. This can be prevented by grounding all involved components and shielding the setup properly, or by applying a 50 Hz notch filter to the signal after it is digitalized. Low frequency interferences from the perfusion system can be introduced to the signal through changes in the fluid level as explained in Section 3.1.4. These interferences can be removed by adjusting the position of the perfusion cannulas and ensuring that the flow of the perfusion is laminar. They can also be filtered out with a digital high pass filter, since most signal shapes of interest are comprised of much higher frequencies.

Since the perfusion solution is bubbled with oxygen, small gas bubbles may travel through the gap between electrodes and organotypic slice samples, causing sudden changes to the electrical conductivity. This effect can be observed as sudden spikes in the acquired signal, which may be mistaken for spontaneous electrical activity of neurons. These spikes often appear near the position of the influx tube, even when the sample is exchanged. To prevent these misleading interferences, one can reduce the in-between gap by applying more pressure to the slice fixture, leading to an overall increase in conductivity.

Some less significant effects may introduce interferences as well, but are easily compensated. Mechanical vibrations, which can cause changes in the perfusion fluid level, are prevented by positioning the measurement setup in an environment that is free of such disturbances. High frequency noise may be attenuated through digital filtering, small changes to the measurement setup or by optimizing the calibration parameters.

3.4 Electrical Stimulation

By changing the membrane potential of neurons in a sample through electrical stimulation, an experimenter can artificially induce EPSPs, IPSPs and action potentials. This

section will discuss stimulation protocols in more detail and illustrate the required signal shapes and amplitudes for effective neural stimulation.

3.4.1 Stimulus Signals

Different stimuli elicit different responses from a neuronal sample, as explained in Section 2.3. Biphasic current pulses are generally preferred to prevent damage to the stimulation electrode. The leading cathodic (negative) pulse is called the stimulating phase and the subsequent anodic (positive) pulse is the reversal phase. The suppressing effect of the reversal phase can be avoided by introducing a short interphase delay of 100 µs between the pulses [MBJ05].

Amplitude and duration of the stimulation pulse depends on the conductivity between the stimulating electrode and the nearby tissue, as well as the type of tissue that is to be stimulated. The minimal current amplitude required to trigger an action potential depends on the duration of the pulse and vice versa, as given by the strength-duration curve depicted in Figure 2.7.

While the MEA2100 system applies stimuli in the form of voltage and current pulses through the electrodes of the MEA chip directly, the CMOS-MEA5000 system can only output positive voltages. The capacitive nature of the CMOS chips leads to the induction of a current in the electrolyte when a changing voltage is applied to the electrode. A positive voltage ramp induces a positive current pulse and vice versa, as shown in Figure 3.7. The current is proportional to the derivative of the voltage, as described by the voltage/current relationship across a capacitance $i(t) = C \cdot dv(t)/dt$.

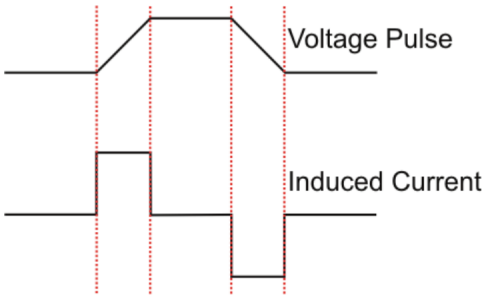

Figure 3.7: The application of a voltage pulse through a CMOS-MEA chip results in the induction of a current pulse in the electrolyte, which is capacitively coupled to the electrode. The image was copied from the *CMOS-MEA5000 System Manual*.

The *MEA Application Note* on *Organotypic Cultures of Hippocampal Slice Preparation* on the website of *Multi Channel Systems* suggests various different stimulation protocols for organotypic samples on MEA chips. For initial testing, biphasic pulses with an amplitude of ±2 V or ±100 µA and a length of 2x 100 µs can be used to find sufficient stimulation sites. The stimulus may be repeated only after 10 s to ensure that the tissue has recovered from previous stimulation. The minimal stimulation amplitude required for effective stimulation can be found by generating an input/output-curve.

To create this curve, the amplitude in a series of pulses is continuously increased in small increments, starting at 500 mV or less, until it reaches 3 V. The amplitude of the signal response is then measured and compared to the input.

3.4.2 Stimulation Sites and Expected Response

An important property of a good stimulation site is that when neurons near it are excited, signals propagate through the tissue along a distinct path. Good stimulation sites for organotypic slice cultures can be found through trial and error by stimulating at multiple different locations and evaluating the response or with the help of visual inspection. Applied stimuli often polarize the electrolyte in the region around the tissue, leading to a wave-like signal propagation across the measurement area. The size of the polarized area depends on the quality of the junction between electrode and sample, and shrinks when the gap between them is decreased.

One frequently used stimulation site in hippocampal slices are the Schaffer Collaterals, which can be easily located under a microscope and serve as a pathway for electrical signals between the CA3 and CA1 region. In intact tissue, when a stimulus is applied near the Schaffer Collaterals, the signal propagates along the nerve fibers and a response can be measured at the CA1 region.

3.4.3 Long-Term Potentiation

After good stimulation sites and the parameters for sufficient stimulation pulses have been identified, they may be applied in quick succession to elicit LTP. Some experiments utilize pulse trains, where pulses are applied at a frequency of 100 Hz over one second, which may lead to short-term LTP. The application of multiple pulse trains of 100 Hz over a period of 10 min leads to the induction of long-term LTP, which can last for several hours under the right conditions. The resulting strengthening of synaptic connections manifests in an increased EPSP amplitude and slope, which can be measured and analyzed.

3.5 Data Analysis

The data generated during MEA measurements may be analyzed with *Matlab* and other computing environments, or with the programs provided by Multi Channel Systems, which are specifically designed for each type of MEA system. The *CMOS-MEA-Tools* software package is suitable for data from the CMOS-MEA5000 and the MEA2100 uses a program called *Multi Channel Analyzer*. They utilize numerous tools to display data and implement signal filtering as well as data processing in a convenient graphical user interface. In *Matlab*, most of these functionalities would have to be programmed by

hand or with the help of dedicated toolboxes, but the user has more liberties regarding the handling of data.

3.5.1 Filtering

Various digital filters can be implemented to remove unwanted noise and interferences from recorded signals. Low pass filters remove low frequency noise caused by the perfusion system, while high pass filters are utilized to attenuate electromagnetic interferences. A notch filter may be used to remove 50 Hz noise coupled into the system from the power lines. All of these filters can be adjusted to different filter orders and types, depending on the required degree of attenuation and the relevant frequency range.

Filters may also be used to split a signal into its individual components like local field potentials (LFPs) and spike activity. LFPs are usually separated out with 300 Hz low-pass Butterworth filters, removing spikes and noise with higher frequencies. A band-pass Bessel filter, which removes frequencies outside of 300 to 3000 Hz, can be employed to remove LFPs and high frequency noise so that spike activity can be analyzed separately. [ODB+15]

3.5.2 Signal Assessment and Spike Detection

Before drawing any conclusions from the recorded data, signal components need to be visually assessed to determine where they originate from. Spikes can be detected with various algorithms and separated into neuronal spikes and artifact waveforms based on their amplitude and timing. Once identified, artifacts caused by noise need to be sorted out by hand, removed through filtering or eliminated with the help of appropriate algorithms.

For the implementation of a simple spike detection algorithm, lower frequency signals need to be filtered out so that spikes may be easily distinguished from the much lower noise level. The baseline noise level can be calculated as the root mean square of the filtered signal. Every spike above a certain threshold, which is usually the baseline noise level multiplied by five [ODB+15], is then detected as shown in Figure 3.8. Due to the occurrence of falsely detected spikes, this process needs to be supervised by the user who can manually adjust the threshold to an optimal value [TIF12].

The shape of neuronal spikes varies between different types of tissue and even single neurons in a sample, but they usually last for around one millisecond. The amplitude of the measured signal is different for individual measurement systems and depends on the conductivity between electrode and sample. Therefore, one can only observe spike amplitudes in relation to other spikes from the same measurement.

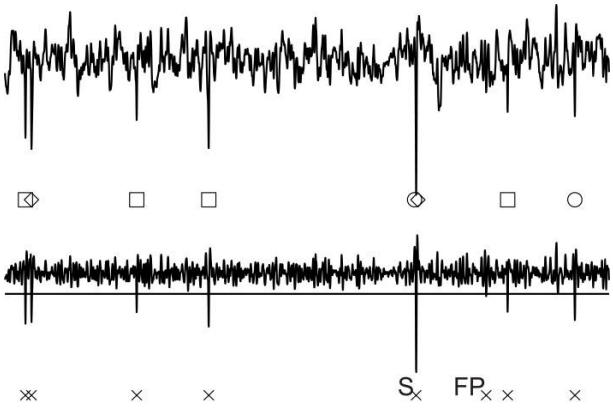

Figure 3.8: Spike detection from simulated raw data [TIF12]. (top) The raw signal with spikes originating from three different neurons (squares, diamonds and circles). (bottom) High-pass filtered signal with the spike detection threshold shown as a horizontal line. The label S marks two synchronized spikes that were detected as a single spike, while FP signifies a falsely detected spike.

Stimulation artifact spikes are often much quicker and show significantly higher amplitudes than spontaneous spikes. They can be detected and removed according to these parameters, or systematically when the stimulation pattern is known. While artifacts caused by perfusion bubbles show up in different shapes and sizes, they frequently originate from the same area. The elicited signal propagates evenly through the entire measurement area, independent of the properties of the tissue. Therefore, these artifacts can be ruled out by observing the propagation pattern and marking them accordingly.

3.5.3 Parameters of Interest

Several parameters of interest can be extracted from recorded MEA data. Spike amplitudes are usually measured as the difference between the maximum and the minimum value of the spike. The frequency of spontaneous activity is determined by counting the occurrence of spikes over a certain time interval. EPSP slopes can give information about the strength of a synaptic connection, which is of great interest in LTP experiments.

Often times, researches add inhibitors to the sample in order to mitigate the activation of certain synaptic receptors or ion channels. These procedures make it possible to observe various neuronal activities independent of each other. For example, in some experiments the neuronal samples are bathed in solutions containing tetrodotoxin, which is known to block the evoked release of neurotransmitters. Therefore, activity through the spontaneous release of quantal packets of neurotransmitter can be observed in isolation [She90].

3.5.4 Signal Propagation

The spatial propagation of a signal in MEA measurements of organotypic samples depends on the signal pathways within the tissue and the conductivity between the electrodes and neurons of the sample. LFPs travel along existing neuronal pathways in the slice culture and the measured signals are ideally confined to a small area surrounding that path. If the conduction between electrodes and neurons is insufficient, electrical signals may spread through the extracellular fluid instead.

The distance a signal travels through the electrolyte is proportional to the conductivity between electrodes and tissue. The electrode contact can be increased by pushing the sample down with a slice fixture, effectively shrinking the gap between them. Therefore, electrical signals are forced to propagate through the neurons in the tissue instead of the electrolyte.

3.5.5 Overflow Artifact Removal

Due to errors in the calibration of CMOS-MEA chips, most notably when there is no reference electrode connecting the perfusion bath to ground, an additional type of interference may occur. The CMOS-MEA5000 system records signals at a voltage resolution of 1 nV and stores the recorded values in a two's complemented 16-bit integer. This leads to problems when a value exceeds the range of $-32\,768$ to $32\,767$ nV. Any values above that threshold get offset to the lower end of the range and vice versa for values below the threshold. These interferences are henceforth referred to as *overflow artefacts*.

In general, overflow artifacts can be prevented by properly adjusting the measurement setup before calibration or by changing the parameters of the calibration. However, data that has already been gathered under these circumstances may be restored with a simple algorithm. Figure 3.9 shows an example signal, where overflow artefacts were identified. The data point may suddenly "jump" to the opposite end of the range when the previous value is near the positive or negative threshold. In between these "jumps", the signal returns to the threshold value, and the data point is lost.

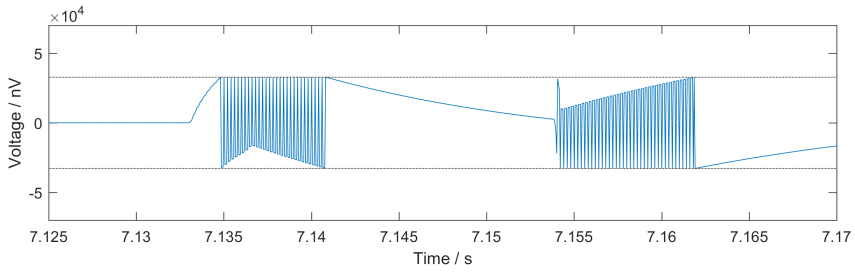

Figure 3.9: Overflow artifacts identified in a signal acquired by the CMOS-MEA5000 system.

Therefore, data recovery has to be carried out in two steps. First, values that are offset need to be identified and shifted back to their original position as shown in Figure 3.10A. The lost values in-between can then be approximated by calculating the average of the previous and the following value. This leads to the signal depicted in Figure 3.10B, where the overflow artifacts have been completely removed. The depicted algorithm for the removal of overflow artifacts was implemented in *Matlab* and can be found in Appendix A.3.

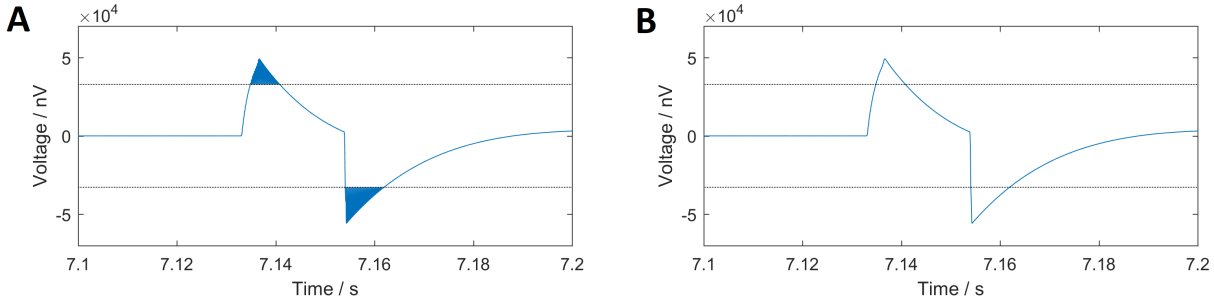

Figure 3.10: Removal of overflow artefacts in two steps. (A) Offset values are identified and shifted back to their original position. (B) Lost data points are recovered by averaging the preceding and the subsequent values.

3.5.6 Spike Sorting

Single neuronal units can be automatically identified in the data measured with an MEA system with the help of powerful spike sorting algorithms. The *CMOS-MEA-Tools* software uses an integrated spike sorter tool based on the algorithm presented in [LWZ16]. The chip area is separated into regions of interest (ROIs), which are spatially connected areas with a higher probability of spike occurrences. The spikes in these regions are then processed for further analysis.

Spike shapes differ from neuron to neuron and can be identified through various algorithms. The built-in spike sorting algorithm of the *CMOS-MEA-Tools* software employs principal component analysis (PCA) to estimate the number of neurons in a ROI. Independent component analysis (ICA) is then used to separate the signals from different neuronal sources. For better performance, calculations can be executed for several or all ROIs in parallel. The algorithm scans the signal from each electrode for different shapes and traces spikes back to the neurons they originate from. A detailed description of this algorithm can be found in the *CMOS-MEA5000-System Manual*.

The result of these calculations is a heatmap of the chip area, where regions with signal generating neuronal units are indicated. For a dataset of 30 s length gathered from 4225 electrodes at a sample rate of 20 kHz, however, this process can take up to several hours and requires the use of specialized computers.

4 Results

The main focus of this thesis was to establish a functioning setup for measurements with MEA systems. Therefore, several experiments with small changes to the setup were conducted to analyze various sources of error and signal artifacts with the aim to eradicate them. Some of these experiments are presented in this chapter, however, many of the emerged issues have yet to be solved and improved upon.

4.1 Measurement Setup

The MEA measurement setup, as described in Section 3.1, went through several small changes throughout the course of this thesis work. The main components of the system, however, remained the same and the initial laboratory setup was arranged as shown in Figure 4.1. Due to a recent collaboration with the Medical University of Graz (MUG), the measurement system was set up in a laboratory of their Center for Medical Research (ZMF).

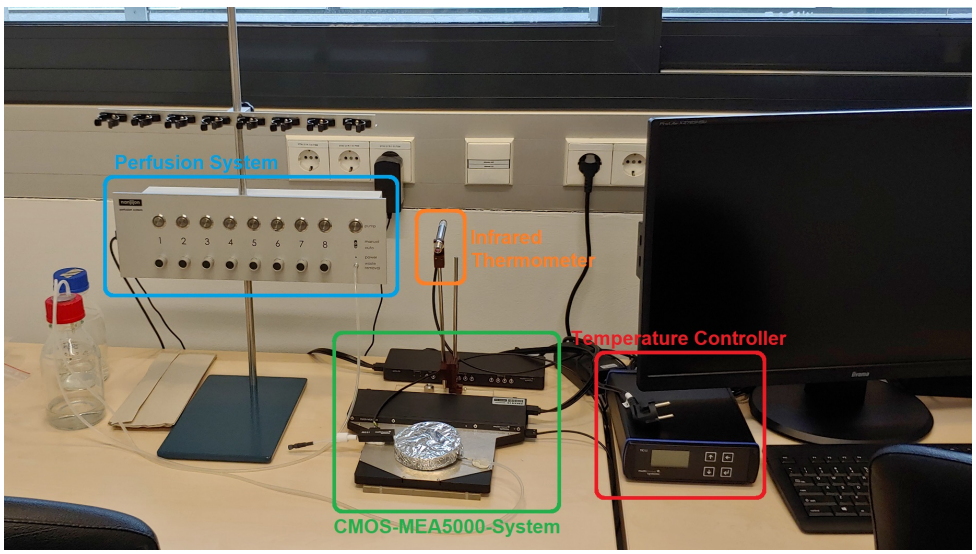

Figure 4.1: Setup for CMOS-MEA measurements. The CMOS-MEA5000 system and the accompanying headstage, the temperature controller connected to the heating perfusion cannula and the heating plate of the MEA system, the infrared thermometer and the perfusion system with the waste container next to it are shown.

4.1.1 Devices and Instruments

The measurement setup consisted of a perfusion system by *Nanion Technologies*, an infrared thermometer (OPTCS-TCLT15 by *Optris*) and a TC02 temperature controller and CMOS-MEA5000 system by *Multi Channel Systems*. The temperature controller was connected to the heating plate of the CMOS-MEA5000 and a perfusion cannula with an integrated continuous-flow heater (PH01 by *Multi Channel Systems*). In later experiments, the MEA2100 system (also by *Multi Channel Systems*) was used instead of the CMOS-MEA5000, which uses the same connector to the headstage and the temperature controller.

In order to be able to inspect samples visually, they were viewed under a reflected-light microscope (BX51 by *Olympus*) with a *CoolLED* pE-300 lighting system. Pictures of samples were taken with a ProgRes Gryphax microscope camera by *Jenoptik*.

4.1.2 Perfusion System

The ACSF buffer used as the perfusion solution was prepared and bubbled beforehand and filled into a reservoir that was suspended above the measurement system. A sealable opening at the bottom of the reservoir was connected to a series of tubes that guided the liquid to the heating cannula and finally into the culture chamber of the MEA chip to supply the sample with a suitable extracellular fluid. The active pump of the Nanion perfusion system then removed the perfusion solution from the culture chamber through suction, after which it was collected in a waste container.

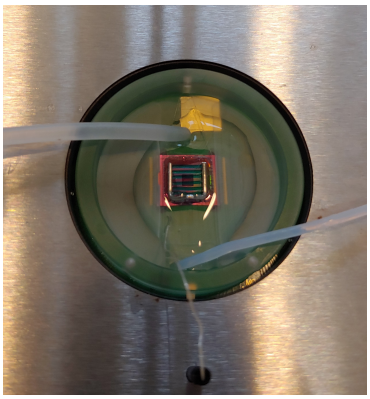

Figure 4.2: CMOS-MEA32-SCA chip with grooves for laminar perfusion flow. The influx tube (top) and the suction tube (bottom) were positioned to achieve a consistent fluid level. A slice grid was placed on top of the organotypic sample and one end of the reference electrode was positioned in the bath.

Figure 4.2 shows the position of the tubes and the reference electrode relative to the culture chamber of a CMOS-MEA32-SCA chip. A slice fixture was placed on top of an organotypic sample in the center of the measurement area. The tubing was held in place and could be adjusted with the help of adhesive pads. The slice fixture

consisted of nylon threads that were glued to a horseshoe-shaped frame made out of biocompatible platinum wire. The frame was bent in a way that a small opening on one side would ensure that the perfusion could freely flow across the sample. Small grooves in the culture chamber of the chip would guide the liquid to achieve laminar flow. The reference electrode was connected to the grounding plane of the CMOS-MEA5000 system and positioned so that its other end was always submerged in the bath.

Due to inconsistencies with the positioning of the perfusion tubes between measurements, 3D-printed fixtures were designed and implemented as shown in Figure 4.3. The perfusion tubes were guided towards the culture chamber of the MEA chip through holes in these fixtures that were held in place with adhesive pads. They allowed for an easier adjustment of the influx and suction tubes to achieve a steady fluid level and reduce perfusion noise.

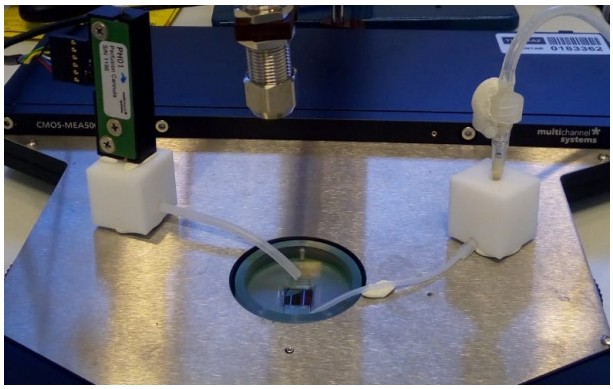

Figure 4.3: Perfusion setup for the CMOS-MEA5000 system to achieve a consistent perfusion flow between measurements and reduce noise.

4.1.3 Organotypic Samples

Samples were kindly prepared, maintained and provided by the researchers at the Center for Medical Research. These samples were mostly organotypic hippocampal and cortical slices, which had been obtained from P5 Sprague Dawley rats. They were placed on a semipermeable membrane in a 6-well plate and stored in an incubator at 37 °C with 5 % CO_2.

4.1.4 Experimental Procedure

Before every measurement, a clean CMOS-MEA chip was mounted in the CMOS-MEA5000 system and the position of the perfusion tubes as well as the reference electrode were adjusted. Optionally, the chip was sometimes coated with a nitrocellulose solution to increase the biocompatibility of the measurement surface. The culture

chamber was filled with a small amount of perfusion solution to serve as a bath for the reference electrode. The sensor area was then covered with an opaque lid for several minutes, after which the automatic chip calibration could be started.

Meanwhile, the 6-well plate with the tissue slices was taken out of the incubator and a small patch of membrane cut out around a selected sample with a scalpel. After the calibration was completed successfully, the perfusion solution was removed and the sample transferred to the electrode area of the MEA chip. The slice grid was placed on top of the sample and, if necessary, held in place with additional weights. Subsequently, the perfusion flow had to be started as quickly as possible to prevent cell death.

The setup for measurements with the MEA2100 system is largely the same except for the calibration step, which is not required for this device. The associated software for data acquisition and recording is called *Multi Channel Experimenter*.

4.2 Data Acquisition

After the setup was complete, data acquisition could be initiated and carried out with the *CMOS-MEA-Tools* software for the CMOS-MEA5000 system. For each new sample, spontaneous activity was observed first to assess the quality of the signal. If necessary, small adjustments to the measurement setup, such as repositioning the perfusion tubes or the reference electrode, were made. When the signal quality was sufficient and the sample showed interesting activity, data was recorded for further analysis. After that, stimulation pulses could be applied to observe the evoked activity of the sample. The signal recordings showcased in this section were all acquired with the CMOS-MEA5000 system.

4.2.1 Signal Recording

Some examples of recorded signals from hippocampal and cortical slice cultures are shown in Figure 4.4. These datasets were acquired without a reference electrode in the perfusion bath. Therefore, they exhibited a much smaller signal amplitude and overflow artifacts, which had to be removed afterwards through signal processing. The signals in the top and center row of the figure were recorded from hippocampal samples and the signal in the bottom row stems from an organotypic cortical slice. The diagrams show evoked and spontaneous activity from initially unknown sources.

The signal in the top row of Figure 4.4 was recorded directly after a biphasic stimulation pulse, leading with the positive phase, was applied to the sample through a 10 by 10 area of electrodes approximately 500 µm away from the recording site. The pulse had a duration of 2x 100 µs with an interphase delay of 100 µs and an amplitude of ± 2 V. The recorded spike is a stimulation artifact that emerged simultaneously with the stimulating pulse and is explained in more detail in Section 4.3.3.

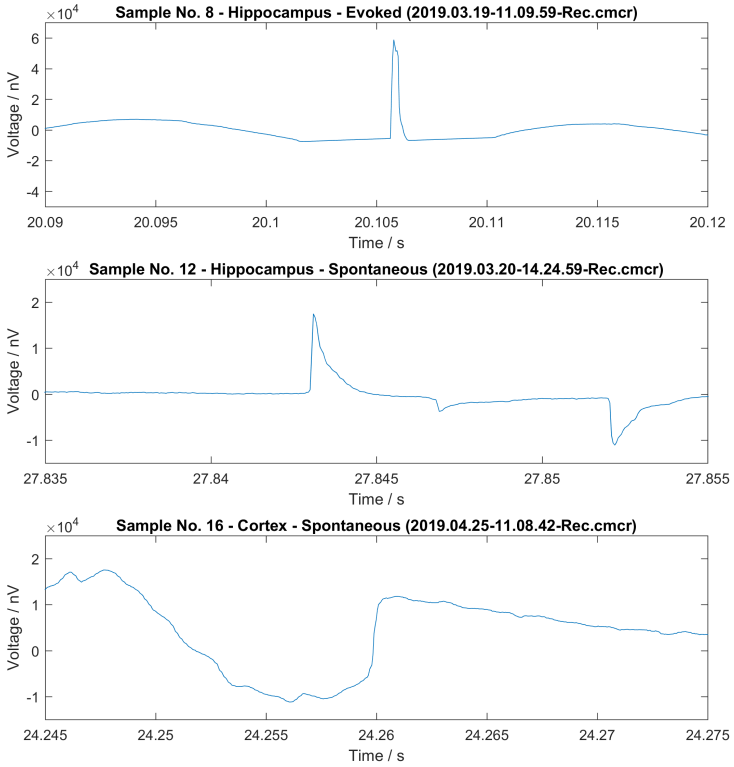

Figure 4.4: Examples of signals measured with the CMOS-MEA5000 system. (top) Evoked activity from a hippocampal slice. The depicted spike occurs start simultaneously with the rising flank of the stimulating pulse. (center) Spontaneous activity from an unknown source measured from a hippocampal sample. (bottom) Spontaneous activity acquired from a cortical slice culture.

4.2.2 Wave Propagation

Electrical activity of the sample can be viewed in the form of a heatmap in the overview window of the *CMOS-MEA-Control* software. Isolated spikes and waves propagating across the chip area can be observed.

One exemplary recording, where a polarizing wave propagated across the chip area, is shown in Figure 4.5. Again, no reference electrode was connected to the system and overflow artifacts had to be removed. In order to achieve this, the overflow artifact removal algorithm had to be applied to the data acquired from every single one of the 4225 electrodes individually. The result was stored in a file structure that could be opened by the *CMOS-MEA-Tools* software. Due to the high number of electrodes, this process took several hours to complete.

To demonstrate the temporal change of the signal, pictures of the heatmap were taken every 5 ms and arranged in a table. During this recording, the area at the top left, which is indicated as a square, was stimulated every 10 s. The depicted polarizing wave, however, emerged approximately 3 s after the previous stimulation pulse. The wave seemingly propagates from the top and left regions towards the center and finally to bottom the right of the measurement area.

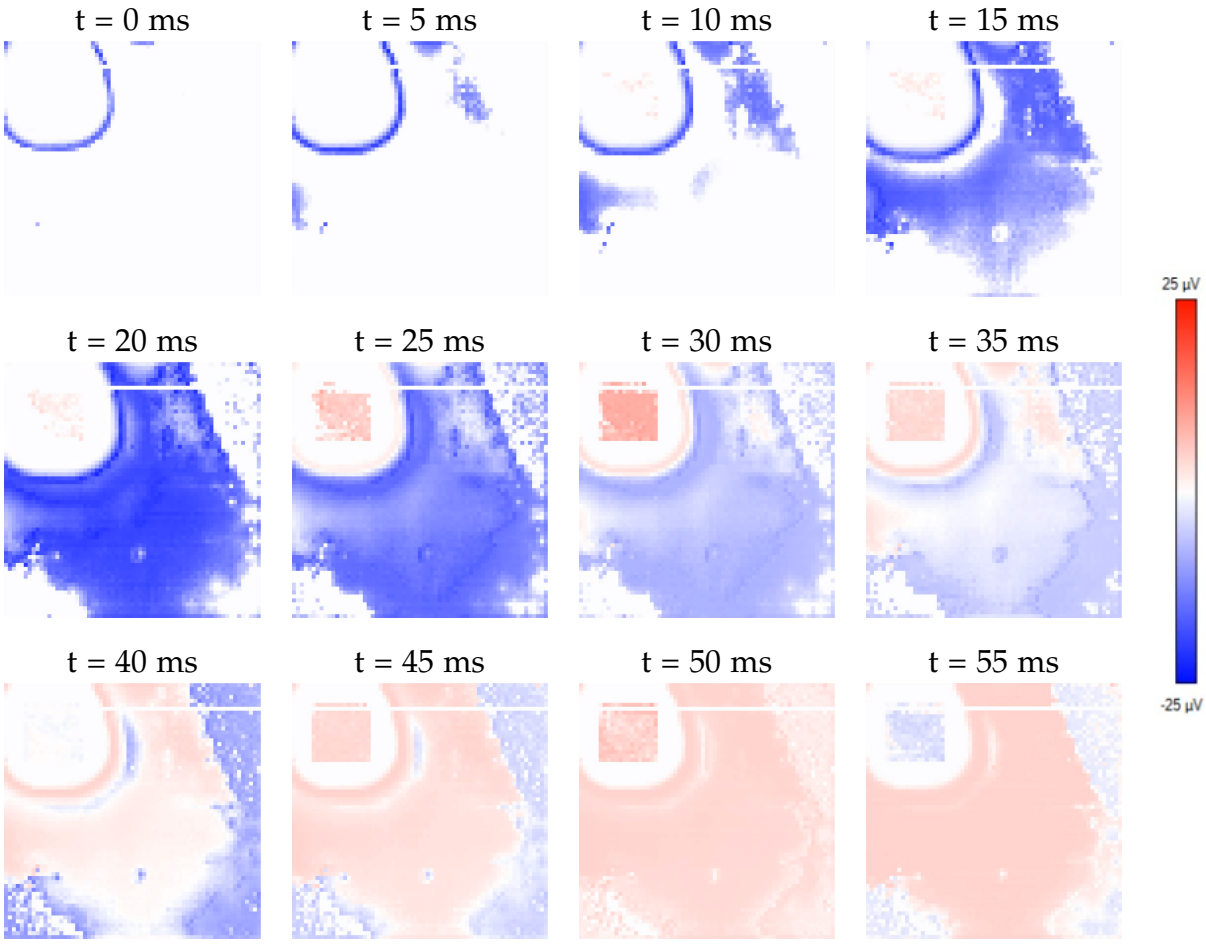

Figure 4.5: Heatmaps showing wave propagation across the measurement area. Pictures were taken in 5 ms intervals. The signal propagates roughly from the top left to the bottom right of the area. The square region on the top left was selected for periodic stimulation, however, no stimulation occurred during the shown time period. The white line at the top presumably originates from a poor electric contact between one pad of the CMOS-MEA chip and the measurement system.

Figure 4.6 depicts the signal acquired at the center of the measurement area at electrode (33,33). The dotted lines mark the beginning and the end of the time interval shown in Figure 4.5. The repolarization and subsequent depolarization of the chip area can be observed.

4.3 Noise and Artifacts

Several different artifacts and noise sources were identified in signals that were measured with the CMOS-MEA5000 system. Some of these signals are depicted in this section and can be used as a reference to evaluate generated data. Overflow artifacts, which may occur when there is no reference electrode connected between the ground

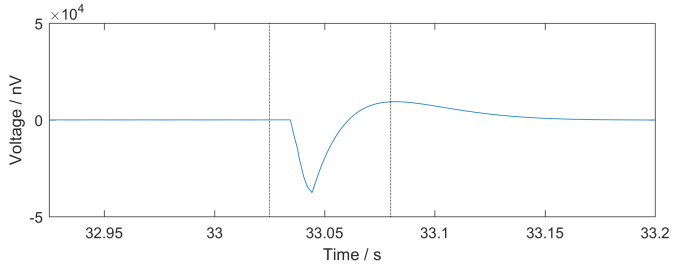

Figure 4.6: Signal acquired at the center electrode (33,33) of the measurement area. The corresponding heatmaps are shown in Figure 4.5. The dotted lines indicate the beginning and end of the time interval observed in these heatmaps.

of the system and the perfusion bath, were already shown and explained in more detail in Section 3.5.5.

4.3.1 Bubble Artifacts

So-called bubble artifacts emerged whenever a gas bubble in the perfusion solution flowed through the gap between the sample and the electrode surface. The resulting change in conduction could be seen in the measured signal as a pair of successive spikes of different polarization. Through squeezing and releasing the perfusion influx tube, these artifacts may be introduced intentionally. An example of a recorded bubble artifact is depicted in Figure 4.7.

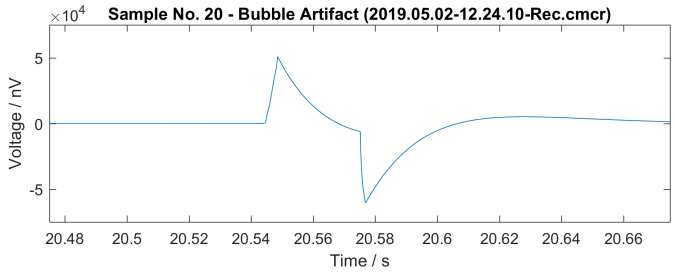

Figure 4.7: Recording of a bubble artifact that was intentionally introduced to the measurement area.

For this measurement, a cortical slice that otherwise showed little to no spontaneous activity had been placed on the electrode area. Overflow artifacts were removed from the signal to get a clear view of its actual shape. Bubble artifacts could be removed by reducing the gap between the sample and the measurement electrodes by holding the sample down with heavier weights. However, no consistent solution to this issue could be established over the course of several experiments.

4.3.2 Power Line Noise

When the MEA system or the perfusion bath were not grounded properly, noise caused by the surrounding power lines was visible in some of the acquired signals. An example recording where a 50 Hz sine signal was modulated onto a measurement electrode is shown in Figure 4.8.

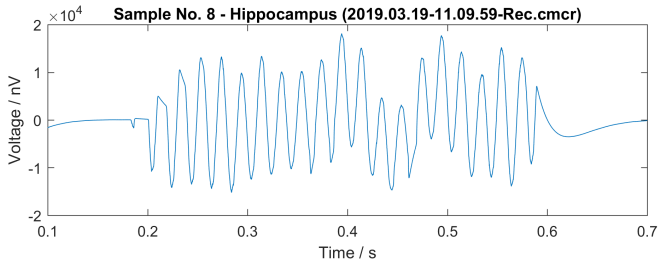

Figure 4.8: 50 Hz power line noise coupled onto a signal recorded with the CMOS-MEA5000 system.

This effect only persisted for short periods of time and in seemingly random intervals. Further investigation showed that these noise intervals seemed to correlate with the noise of the suction tube of the perfusion system. The power line noise was reduced substantially when a reference electrode was added to the setup.

4.3.3 Stimulation Artifacts

Whenever a stimulation pulse was applied to a sample during experiments conducted with the CMOS-MEA5000 system, the entire measurement area was briefly polarized. This was likely caused by the fact that the perfusion solution served as conducting medium for the electrical stimulus. An example of a stimulation artifact is shown in Figure 4.9.

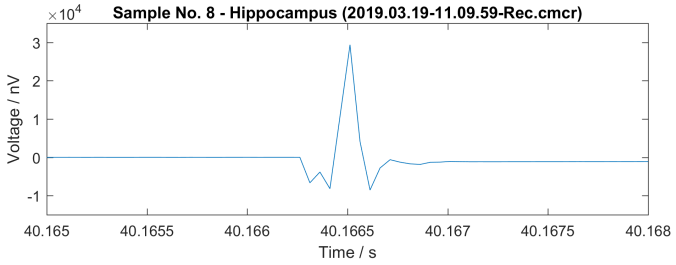

Figure 4.9: Example of a stimulation artifact emerging directly after the application of a stimulating pulse.

The depicted spike arose directly after the start of the rising slope of a stimulus applied to an area consisting of 10 by 10 electrodes 500 µm away from the recording site. The stimulus was adjusted to have a rising and falling slope with a duration of 100 µs each, an interphase delay of 100 µs and an amplitude of 2 V.

Spikes caused by evoked activity should only emerge several milliseconds after a stimulation pulse. Stimulation artifacts, however, seem to occur simultaneously. These artifacts could therefore be removed systematically with the help of an algorithm, if the timing of the stimulus is known. Due to their comparatively low period duration of approximately 0.5 ms, filtering could also be utilized to attenuate the amplitude of the artifact spike. Another solution would be to increase the conduction between the measurement electrodes and the sample. The electrical signal caused by stimulation would be forced to flow through the sample instead of the perfusion solution, preventing the occurrence of stimulation artifacts in advance. This could, for example, be achieved by applying common coating protocols to the culture chamber of the MEA chip, through which the sample may stick directly to the electrode surface.

4.4 Signal Processing

Further processing of recorded signals was carried out with *Matlab*. In order to look at possible LFPs without higher frequency disturbances, low-pass filters were utilized. High-pass filters were applied to remove signal drifts and observe spikes in isolation.

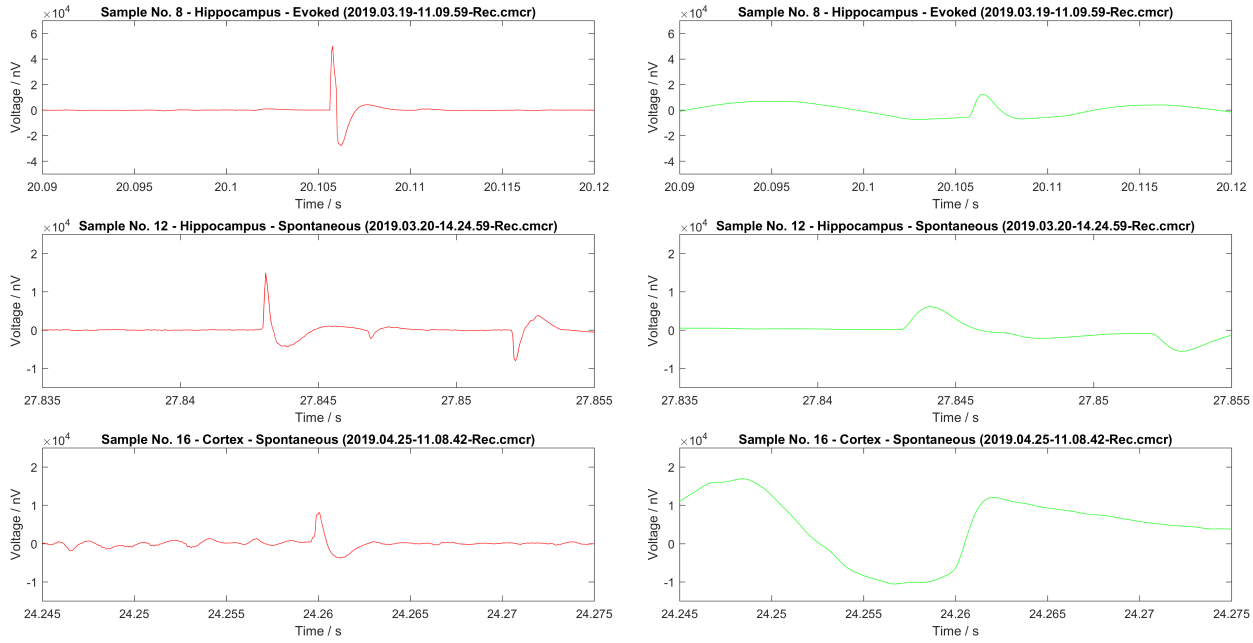

Figure 4.10: The signals shown in Figure 4.4 were processed for further analysis. (left column) A 2nd-order Bessel high-pass filter with a corner frequency of 300 Hz was applied. (right column) Filtering with a 2nd-order Buttworth low-pass filter with a corner frequency of 300 Hz.

Figure 4.10 shows the same data that was depicted in Figure 4.4 with different filters applied to the signal. The signal shape shown on the left (red) was processed with a digital 2nd-order Bessel high-pass filter with a corner frequency of 300 Hz. In the diagrams on the right (green), a 2nd-order Butterworth low-pass filter was applied to

the original signal to remove frequency components above 300 Hz. It is apparent that only spikes remain on the left side, while the right column shows signal drifts and possibly underlying LFPs in the signals.

5 Discussion

5.1 Measurement Setup Challenges

Several major challenges regarding the measurement setup occurred over the course of the experiments conducted for this thesis. Due to an initial misconception about the requirement of a reference electrode for different MEA systems, measurements were carried out without a reference electrode in the beginning. Automatic calibration of the CMOS-MEA chips was successful in some cases. The measured signals, however, showed a much lower signal amplitude than expected and were disturbed by overflow artifacts. Due to these overflow artifacts, spike sorting of the acquired data yielded no meaningful results since the sudden "jumps" in the signal were detected as spikes as well.

Another major problem was due to limitations regarding the bubbling of the ACSF buffer. Initially, only pure oxygen was available in the laboratory with the measurement setup and an alternative buffer solution with HEPES as a base had to be used. Only much later in the experiments, a carbogen gas source was installed in the laboratory for the use of bicarbonate-based buffers that were suggested in the *MEA Application Notes*. However, due to the positioning of the measurement setup in the laboratory, it was impossible to continuously bubble the ACSF buffer during measurements. The buffer solution therefore had to be bubbled ahead of time and transferred to the perfusion reservoir right before it was used. Hence, the supply of oxygen to the sample may have been inefficient and possibly insufficient for the cells to survive. Positioning and adjustment of the perfusion system proved difficult as well, but was made easier through the usage of 3D-printed guides for the perfusion tubes, which were designed and provided by a colleague at the TU Graz.

The fixation of organotypic samples posed another problem. It was difficult to find a consistent method to hold the slices down during the measurement. This lead to an additional issue, since air bubbles could travel through the gap between the MEA chip and the sample, leading to spike-shaped interferences due to the changing conductance. Several different approaches with weights and 3D-printed fixtures to place on top of the slice grid were tested, but it was eventually decided that employing a micromanipulator would be unavoidable to achieve reproducible results.

In later stages of the experiments, a reference electrode was used. From then on, the automated calibration of CMOS-MEA5000 chips was mostly successful and the system was more stable to external noise sources. However, satisfactory signals could still not

be measured. It was speculated that the cells in the samples either did not survive the transfer to the MEA chips, or died shortly after due to the poor biocompatibility of the chip or the insufficient oxygen supply.

Measurements with the MEA2100 system suffered from the same problems as the CMOS-MEA5000 system and it was concluded that the problems must originate from their common denominator, the perfusion system. It was therefore reasoned that a different approach for the perfusion was needed and, if possible, the requirement of an active perfusion system would have to be eliminated entirely.

5.2 Signal Evaluation

Initially, several datasets showing spontaneous and evoked spikes were recorded and evaluated. It was soon apparent, however, that it was unclear which source these signals originated from. Overflow artifacts were identified and had to be removed through additional processing. To prevent these artifacts, the use of a reference electrode became inevitable.

Even then, spikes were difficult to categorize. Bubble artifacts were introduced intentionally and found to exhibit very similar amplitudes and timings to previously measured signals that were thought to be spontaneous spikes generated by neurons. Stimulation in one small region of the chip caused the polarization of the entire measurement area and the evoked spikes emerged simultaneously with the stimulation pulse. Therefore, it seemed that the signal was conducted through a different medium than the sample itself, namely the extracellular ACSF solution. To solve this problem, more pressure was applied to the slice fixture to decrease the in-between gap, however, no consistent results could be achieved.

The acquired data depicted in Figure 4.5 shows that the measurement of propagating waves is possible in principle. However, it cannot be said with certainty where these signals originate from since the effect could not be reproduced. The waveform could either be caused by an air bubble moving across the measurement area or come from a neuronal EPSP. The latter would be likely, since the waveform exhibits very similar timing and shape as the signal recorded from the MEA2100 signal generator test chip depicted in Figure 3.6A.

6 Conclusion and Outlook

A theoretical framework for MEA measurements was composed with the help of various literary sources. Several studies that relied on the use of MEA systems were found and reviewed. The measurement system was set up and two different MEA systems were used for experiments. Small changes to the measurement setup were tested and adapted with the aim to make it function properly and optimize its operation. Many challenges with MEA measurements of electrophysiological signals were identified and solutions for recurring problems proposed. A general foundation for future MEA measurements was established and compiled.

Unfortunately, no meaningful signals could be acquired from experiments with more than 30 organotypic hippocampal and cortical samples. However, many of the issues could be solved with the now established knowledge about the measurement system and its components. A micromanipulator could be used to hold the slice down during measurements and eliminate bubble artifacts and stimulation artifacts. Chip coating would help to increase the biocompatibility of the electrode surface as well as the electrical conduction between sample and electrodes. Continuous bubbling of the ACSF buffer solution while it remains in the perfusion reservoir might be inevitable to prevent cell death. Different buffer solutions could be tested and may yield better results.

One of the next steps could be to utilize a patch clamping system, which was established to work properly, simultaneously with an MEA system. That way, the experimenter could verify if the absence of spikes is caused by an insufficient contact between sample and measurement electrodes of the MEA chip or stems from the fact that the cells are already too damaged to produce any signals.

Another approach would be to test the system with dissociated neuronal samples, which do not require a perfusion system, before returning to measurements with organotypic slice cultures. Thereby, moving parts in the system could be eliminated to achieve more consistent results. It would not be subject to problems arising from the movement of the sample, the composition of the perfusion solution or the introduction of bubble artifacts. The same would hold true for organotypic samples grown directly on the MEA chips, which require a more complex storage solution. By establishing a working system with these types of samples, the sources of error for MEA measurements could be narrowed down. The resulting knowledge could later be applied to experiments with organotypic slices with a perfusion system.

Appendices

A.1 ACSF Buffer Solutions

Three examples of different ACSF buffer solutions using bicarbonate or HEPES as a base buffer are shown in Tables A.1, A.2 and A.3.

Compound	Conc. [mM]	M.W.	g/1L 10x Stock	g/2L 10x Stock	g/500mL ACSF	g/1L ACSF
NaCl	125	58.44	73.050	146.100		
KCl	3.5	74.55	2.609	5.219		
$NaH_2PO_4 \cdot 2H_2O$	1.2	156.01	1.872	3.744		
$CaCl_2 \cdot 2H_2O$	2.4	147.01	3.528	7.056		
$MgCl_2 \cdot 6H_2O$	1.3	203.30	2.643	5.286		
$NaHCO_3$	26	84.01			1.092	2.184
Glucose$\cdot H_2O$	25	198.17			2.477	4.954

Table A.1: Bicarbonate ACSF-Buffer from the MEA application note for organotypic cultures (provided by Multi Channel Systems GmbH).

Compound	Conc. [mM]	M.W.	g/1L 10x Stock	g/2L 10x Stock	g/500mL ACSF	g/1L ACSF
NaCl	130	58.44	75.972	151.944		
KCl	3	74.55	2.237	4.473		
$NaH_2PO_4 \cdot 2H_2O$	1.25	156.01	1.950	3.900		
$MgSO_4 \cdot 7H_2O$	1.3	246.47	3.204	6.408		
$CaCl_2 \cdot 2H_2O$	2.5	147.01	3.675	7.351		
$NaHCO_3$	20	84.01			0.840	1.680
Glucose$\cdot H_2O$	10	198.17			0.991	1.982

Table A.2: Bicarbonate ACSF-Buffer from `https://clampthis.files.wordpress.com/2011/10/acsf-recipes.pdf`.

Compound	Conc. [mM]	M.W.	g/1L 10x Stock	g/2L 10x Stock	g/500mL ACSF	g/1L ACSF
NaCl	136	58.44	79.478	158.957		
KCl	2.5	74.55	1.864	3.728		
$MgCl_2 \cdot 6H_2O$	1.3	203.3	2.643	5.286		
$CaCl_2 \cdot 2H_2O$	2	147.01	2.940	5.880		
HEPES	10	238.3			1.192	2.383
Glucose$\cdot H_2O$	10	198.17			0.991	1.982

Table A.3: HEPES ACSF-Buffer from https://clampthis.files.wordpress.com/2011/10/acsf-recipes.pdf.

A.2 CMOS-MEA Measurement Protocol

When recording data with the CMOS-MEA5000 system, related information and parameters of interest should be documented in measurement protocols like the one shown in Figure A.1. For easy reference, selected stimulation sites may be marked in the grid.

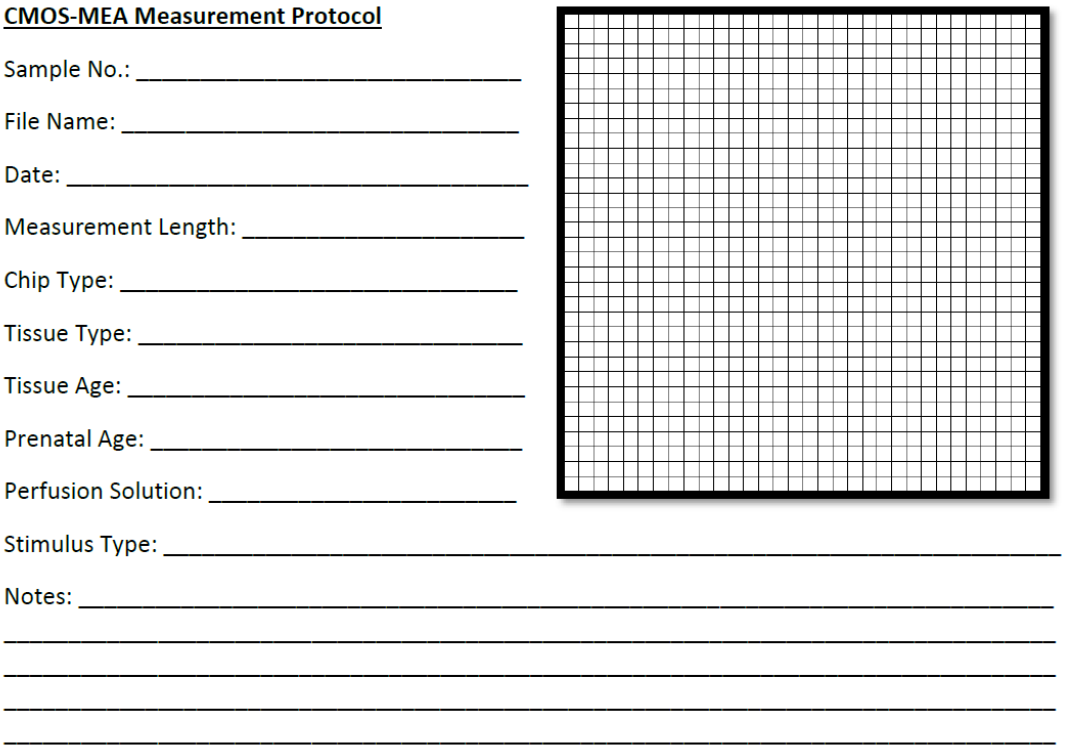

Figure A.1: Protocol for measurements with the CMOS-MEA5000 system.

A.3 Matlab Algorithm for Overflow Artifact Removal

```
%% Function to remove Overflow Artifacts from CMOS-MEA Data
% Inputs: raw signal, detection threshold (in percent of min/max values)

function sig_new = fix_overflow(sig_raw,threshold)

% Max and min values defined by two's complemented 16-bit integer
max_val = 2^15-1;
min_val = -2^15;

offset = max_val-min_val;   % Offset for correction of data points

sig_new(1) = sig_raw(1);    % Assign first value

%% Step 1: identitfy offset values and shift them back to original position

for i = 2 : length(sig_raw)

    % If value above positive threshold and following value negative
    if (sig_new(i-1) >= max_val*threshold) && (sig_raw(i) < 0)
        sig_new(i) = sig_raw(i) + offset;   % Positive shift

    % If value below negative threshold and following value positive
    elseif (sig_new(i-1) <= min_val*threshold) && (sig_raw(i) > 0)
        sig_new(i) = sig_raw(i) - offset;   % Negative shift

    % Do not change signal otherwise
    else
        sig_new(i) = sig_raw(i);
    end
end

%% Step 2: recover lost data by averaging previous and following value

for i = 2 : length(sig_new)-1

    % Identify lost data point at max or min of range
    if (sig_new(i) == max_val) || (sig_new(i) == min_val)

        % Average previous and following value
        sig_new(i) = (sig_new(i-1)+sig_new(i+1))/2;
    end
end

end
```

Bibliography

[AL07] Amaral, D ; Lavenex, P: Hippocampal neuroanatomy. In: *The Hippocampus Book*. 2007, S. 37

[BG13] Brocker, David T. ; Grill, Warren M.: Principles of electrical stimulation of neural tissue. Version: 2013. http://dx.doi.org/10.1016/B978-0-444-53497-2.00001-2. In: *Handbook of Clinical Neurology* Bd. 116. 2013. – DOI 10.1016/B978–0–444–53497–2.00001–2. – ISSN 00729752, S. 3–18

[BVE+15] Bardy, Cedric ; Van Den Hurk, Mark ; Eames, Tameji ; Marchand, Cynthia ; Hernandez, Ruben V. ; Kellogg, Mariko ; Gorris, Mark ; Galet, Ben ; Palomares, Vanessa ; Brown, Joshua ; Bang, Anne G. ; Mertens, Jerome ; Böhnke, Lena ; Boyer, Leah ; Simon, Suzanne ; Gage, Fred H.: Neuronal medium that supports basic synaptic functions and activity of human neurons in vitro. In: *Proceedings of the National Academy of Sciences of the United States of America* 112 (2015), Nr. 20, S. E2725–E2734. http://dx.doi.org/10.1073/pnas.1504393112. – DOI 10.1073/pnas.1504393112. – ISSN 10916490

[Byr14] Byrne, John H.: Postsynaptic Potentials and Synaptic Integration. Version: 2014. http://dx.doi.org/10.1016/B978-0-12-397179-1.00016-6. In: *From Molecules to Networks: An Introduction to Cellular and Molecular Neuroscience: Third Edition*. 2014. – DOI 10.1016/B978–0–12–397179–1.00016–6. – ISBN 9780123971791, S. 489–507

[Com16] Commons, Wikimedia: *File:Action potential.svg — Wikimedia Commons, the free media repository*. https://commons.wikimedia.org/w/index.php?title=File:Action_potential.svg&oldid=194679385. Version: 2016. – [Online; accessed 30-July-2019]

[Com18] Commons, Wikimedia: *File:1225 Chemical Synapse.jpg — Wikimedia Commons, the free media repository*. https://commons.wikimedia.org/w/index.php?title=File:1225_Chemical_Synapse.jpg&oldid=293019337. Version: 2018. – [Online; accessed 26-August-2019]

[CSGR06] Capron, Brigitte ; Sindic, Christian ; Godaux, Emile ; Ris, Laurence: The characteristics of LTP induced in hippocampal slices are dependent on

slice-recovery conditions. In: *Learning and Memory* 13 (2006), Nr. 3, S. 271–277. http://dx.doi.org/10.1101/lm.135406. – DOI 10.1101/lm.135406. – ISSN 10720502

[DB13] Destexhe, Alain ; Bedard, Claude: Local field potential. In: *Scholarpedia* 8 (2013), Nr. 8, S. 10713. http://dx.doi.org/10.4249/scholarpedia.10713. – DOI 10.4249/scholarpedia.10713

[DFG14] Davis, Katherine E. ; Fox, Sarah ; Gigg, John: Increased hippocampal excitability in the 3xTgAD mouse model for Alzheimer's disease in vivo. In: *PLoS ONE* 9 (2014), Nr. 3. http://dx.doi.org/10.1371/journal.pone.0091203. – DOI 10.1371/journal.pone.0091203. – ISSN 19326203

[FEH+09] Frey, U. ; Egert, U. ; Heer, F. ; Hafizovic, S. ; Hierlemann, A.: Subcellular-resolution recording of electrical activity using a CMOS-microelectrode system. In: *TRANSDUCERS 2009 - 15th International Conference on Solid-State Sensors, Actuators and Microsystems*, 2009. – ISBN 9781424441938, S. 1674–1677

[FJ10] Fry, Chris H. ; Jabr, Rita I.: *The action potential and nervous conduction*

[Fle19] Fletcher, Allan: *Action potential: generation and propagation*

[GCD+97] Gähwiler, B. H. ; Capogna, M. ; Debanne, D. ; McKinney, R. A. ; Thompson, S. M.: Organotypic slice cultures: A technique has come of age. In: *Trends in Neurosciences* 20 (1997), Nr. 10, S. 471–477. http://dx.doi.org/10.1016/S0166-2236(97)01122-3. – DOI 10.1016/S0166–2236(97)01122–3. – ISSN 01662236

[HF12] Holz, Ronald W. ; Fisher, Stephen K.: Synaptic Transmission and Cellular Signaling: An Overview. Version: 2012. http://dx.doi.org/10.1016/B978-0-12-374947-5.00012-2. In: *Basic Neurochemistry*. 2012. – DOI 10.1016/B978–0–12–374947–5.00012–2. – ISBN 9780123749475, S. 235–257

[HFY+18] Heard, Matthew ; Ford, Joni ; Yene, Neude ; Straiton, Benjamin ; Havanas, Patrick ; Guo, Liang: Advancing the neurocomputer. In: *Neurocomputing* 284 (2018), S. 36–51. http://dx.doi.org/10.1016/j.neucom.2018.01.021. – DOI 10.1016/j.neucom.2018.01.021. – ISSN 18728286

[Hum15] Humpel, C.: Organotypic brain slice cultures: A review. In: *Neuroscience* 305 (2015), S. 86–98. http://dx.doi.org/10.1016/j.neuroscience.2015.07.086. – DOI 10.1016/j.neuroscience.2015.07.086. – ISSN 03064522

[LBP11] Lein, Pamela J. ; Barnhart, Christopher D. ; Pessah, Isaac N.: Acute hippocampal slice preparation and hippocampal slice cultures. In: *Methods in Molecular Biology* 758 (2011), S. 115–134. http://dx.doi.org/10.1007/978-1-61779-170-3. – DOI 10.1007/978–1–61779–170–3. – ISBN 9781617791697

[LWZ16] Leibig, Christian ; Wachtler, Thomas ; Zeck, Günther: Unsupervised neural spike sorting for high-density microelectrode arrays with convolutive independent component analysis. In: *Journal of Neuroscience Methods* 271 (2016), S. 1–13. http://dx.doi.org/10.1016/j.jneumeth.2016.06.006. – DOI 10.1016/j.jneumeth.2016.06.006. – ISSN 1872678X

[MAA+18] Malerba, Mario ; Amin, Hayder ; Angotzi, Gian N. ; Maccione, Alessandro ; Berdondini, Luca: Fabrication of multielectrode arrays for neurobiology applications. Version: 2018. http://dx.doi.org/10.1007/978-1-4939-7792-5. In: *Methods in Molecular Biology* Bd. 1771. 2018. – DOI 10.1007/978–1–4939–7792–5. – ISSN 10643745, S. 147–157

[MB09] Mortimer, J. T. ; Bhadra, Narendra: Fundamentals of Electrical Stimulation. Version: 2009. http://dx.doi.org/10.1016/B978-0-12-374248-3.00012-4. In: *Neuromodulation* Bd. 1. 2009. – DOI 10.1016/B978–0–12–374248–3.00012–4. – ISBN 9780123742483, S. 109–121

[MBJ05] Merrill, Daniel R. ; Bikson, Marom ; Jefferys, John G.: *Electrical stimulation of excitable tissue: Design of efficacious and safe protocols*

[MTB+01] Muller, Dominique ; Toni, Nicolas ; Buchs, Pierre-Alain ; Nicolas, Dominique ; Parisi, Lorena ; Stoppini, Luc: Interface Organotypic Hippocampal Slice Cultures. In: *Protocols for Neural Cell Culture* (2001), S. 13–27. http://dx.doi.org/10.1385/1-59259-207-4:13. – DOI 10.1385/1–59259–207–4:13. ISBN 978–1–59259–207–4

[ND09] Nault, Francine ; De Koninck, Paul: Dissociated Hippocampal Cultures. Version: 2009. http://dx.doi.org/10.1007/978-1-60761-292-6. 2009. – DOI 10.1007/978–1–60761–292–6, S. 137–159

[ODB+15] Obien, Marie Engelene J. ; Deligkaris, Kosmas ; Bullmann, Torsten ; Bakkum, Douglas J. ; Frey, Urs: *Revealing neuronal function through microelectrode array recordings*

[OKMS16] Odawara, A. ; Katoh, H. ; Matsuda, N. ; Suzuki, I.: Induction of long-term potentiation and depression phenomena in human induced pluripotent stem cell-derived cortical neurons. In: *Biochemical and Biophysical Research Communications* 469 (2016), Nr. 4, S. 856–862. http://dx.doi.org/10.1016/j.bbrc.2015.12.087. – DOI 10.1016/j.bbrc.2015.12.087. – ISSN 10902104

[PRD+09] Per, Andersen ; Richard, Morris ; David, Amaral ; Tim, Bliss ; John, O'Keefe K.: The Hippocampal Formation. Version: 2009. http://dx.doi.org/10.1093/acprof:oso/9780195100273.003.0001. In: *The Hippocampus Book*. 2009. – DOI 10.1093/acprof:oso/9780195100273.003.0001. – ISBN 9780199864133

[PSS+11] Plenz, Dietmar ; Stewart, Craig V. ; Shew, Woodrow ; Yang, Hongdian ; Klaus, Andreas ; Bellay, Tim: Multi-electrode Array Recordings of Neuronal Avalanches in Organotypic Cultures. In: *Journal of Visualized*

Experiments (2011), Nr. 54. http://dx.doi.org/10.3791/2949. – DOI 10.3791/2949

[PXM13] Peng, Yun ; Xiong, Wen C. ; Mei, Lin: Culture of dissociated hippocampal neurons. In: *Methods in Molecular Biology* 1018 (2013), S. 39–47. http://dx.doi.org/10.1007/978-1-62703-444-9-4. – DOI 10.1007/978–1–62703–444–9–4. – ISBN 9781627034432

[RPQ15] Rey, Hernan G. ; Pedreira, Carlos ; Quian Quiroga, Rodrigo: *Past, present and future of spike sorting techniques*

[Sch97] Schulz, Paul E.: Long-term potentiation involves increases in the probability of neurotransmitter release. In: *Proceedings of the National Academy of Sciences of the United States of America* 94 (1997), Nr. 11, S. 5888–5893. http://dx.doi.org/10.1073/pnas.94.11.5888. – DOI 10.1073/pnas.94.11.5888. – ISSN 00278424

[She90] Shepherd, Gordon M.: *The Synaptic Organization of the Brain*. 1990. – 1–580 S. – ISBN 0195062558

[SLMR09] Stegenga, Jan ; Le Feber, Joost ; Marani, Enrico ; Rutten, W. L C.: The effect of learning on bursting. In: *IEEE Transactions on Biomedical Engineering* 56 (2009), Nr. 4, S. 1220–1227. http://dx.doi.org/10.1109/TBME.2008.2006856. – DOI 10.1109/TBME.2008.2006856. – ISSN 00189294

[SM01] Shahaf, G. ; Marom, S.: Learning in networks of cortical neurons. In: *Journal of Neuroscience* 21 (2001), Nr. 22, S. 8782–8788. – ISSN 02706474

[SZI17] Stein, Liana R. ; Zorumski, Charles F. ; Izumi, Yukitoshi: Dissection method affects electrophysiological properties of hippocampal slices. In: *Oruen* 2 (2017), Nr. 3, 94–101. https://www.oruen.com/wp-content/uploads/2017/12/HC-Slices.pdf

[TBT+17] Tidball, Patrick ; Burn, Hannah V. ; Teh, Kai L. ; Volianskis, Arturas ; Collingridge, Graham L. ; Fitzjohn, Stephen M.: Differential ability of the dorsal and ventral rat hippocampus to exhibit group I metabotropic glutamate receptor–dependent synaptic and intrinsic plasticity. In: *Brain and Neuroscience Advances* 1 (2017), S. 239821281668979. http://dx.doi.org/10.1177/2398212816689792. – DOI 10.1177/2398212816689792. – ISSN 2398–2128

[TIF12] Takekawa, Takashi ; Isomura, Yoshikazu ; Fukai, Tomoki: Spike sorting of heterogeneous neuron types by multimodality-weighted PCA and explicit robust variational bayes. In: *Frontiers in Neuroinformatics* 6 (2012), Nr. MARCH. http://dx.doi.org/10.3389/fninf.2012.00005. – DOI 10.3389/fninf.2012.00005. – ISSN 16625196

[VPS+03] Van Bergen, A. ; Papanikolaou, T. ; Schuker, A. ; Möller, A. ; Schlosshauer, B.: Long-term stimulation of mouse hippocampal slice culture on microelectrode array. In: *Brain Research Protocols* 11 (2003), Nr. 2, S. 123–133. http://dx.doi.org/10.1016/S1385-299X(03)00024-2. – DOI 10.1016/S1385–299X(03)00024–2. – ISSN 1385299X

[VWC+04] Van Pelt, Jaap ; Wolters, Pieter S. ; Corner, Michael A. ; Rutten, Wim L. ; Ramakers, Ger J.: Long-term characterization of firing dynamics of spontaneous bursts in cultured neural networks. In: *IEEE Transactions on Biomedical Engineering* 51 (2004), Nr. 11, S. 2051–2062. http://dx.doi.org/10.1109/TBME.2004.827936. – DOI 10.1109/TBME.2004.827936. – ISSN 00189294

[WHG02] Wasling, Pontus ; Hanse, Eric ; Gustafsson, Bengt: Long-term depression in the developing hippocampus: Low induction threshold and synapse nonspecificity. In: *Journal of Neuroscience* 22 (2002), Nr. 5, S. 1823–1830. – ISSN 02706474

[ZJC+17] Zeck, Günther ; Jetter, Florian ; Channappa, Lakshmi ; Bertotti, Gabriel ; Thewes, Roland: Electrical Imaging: Investigating Cellular Function at High Resolution. In: *Advanced Biosystems* 1 (2017), Nr. 11, S. 1700107. http://dx.doi.org/10.1002/adbi.201700107. – DOI 10.1002/adbi.201700107